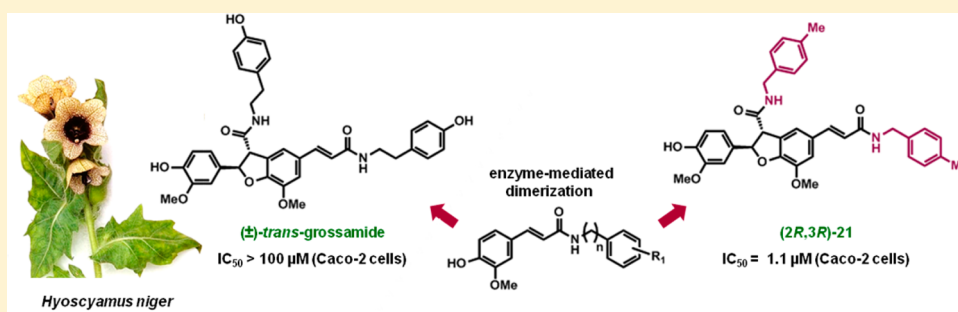


Dihydrobenzofuran Neolignanamides: Laccase-Mediated Biomimetic Synthesis and Antiproliferative Activity

Nunzio Cardullo,[†] Luana Pulvirenti,[†] Carmela Spatafora,^{*,†} Nicolò Musso,[‡] Vincenza Barresi,[‡] Daniele Filippo Condorelli,[‡] and Corrado Tringali[†]

[†]Dipartimento di Scienze Chimiche and [‡]Dipartimento di Scienze Biomediche e Biotecnologiche, Sezione di Biochimica Medica, Università degli Studi di Catania, Viale A. Doria 6, I-95125 Catania, Italy

S Supporting Information



ABSTRACT: The biomimetic synthesis of a small library of dihydrobenzofuran neolignanamides (the natural *trans*-grossamide (4) and the related compounds 21–28) has been carried out through an eco-friendly oxidative coupling reaction mediated by *Trametes versicolor* laccase. These products, after complete spectroscopic characterization, were evaluated for their antiproliferative activity against Caco-2 (colon carcinoma), MCF-7 (mammary adenocarcinoma), and PC-3 (prostate cancer) human cells, using an MTT bioassay. The racemic neolignanamides (±)-21 and (±)-27, in being the most lipophilic in the series, were potently active, with GI_{50} values comparable to or even lower than that of the positive control 5-FU. The racemates were resolved through chiral HPLC, and the pure enantiomers were subjected to ECD measurements to establish their absolute configurations at C-2 and C-3. All enantiomers showed potent antiproliferative activity, with, in particular, a GI_{50} value of 1.1 μM obtained for (2*R*,3*R*)-21. The effect of (±)-21 on the Caco-2 cell cycle was evaluated by flow cytometry, and it was demonstrated that (±)-21 exerts its antiproliferative activity by inducing cell cycle arrest and apoptosis.

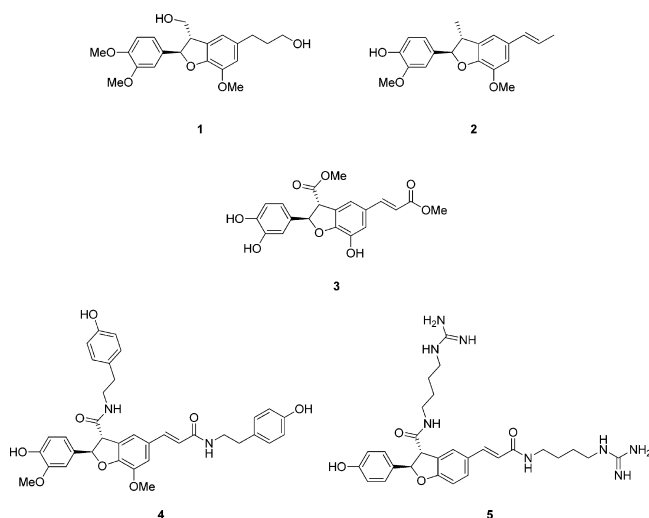
One of the reasons for the renewed interest in small molecules of natural origin is their structural diversity, which, as the result of millions of years of evolution, affords selected molecules with biological properties that are advantageous for the organism producing them. A clear example of this is the family of lignans, as well as related compounds (neolignans, oxylignans, and mixed lignans), distributed widely within the plant kingdom, which have an extraordinary variety of structures and biological properties. These compounds share a common origin from the shikimate pathway, but different biosynthetic mechanisms, normally through oxidative coupling of two phenylpropanoid (C_6C_3) units, lead to remarkably different carbon skeletons. According to the IUPAC recommendations,¹ the term “lignan” refers to a dimer generated by a β – β' (8–8') oxidative coupling of two propylbenzene residues, whereas the term “neolignan” should be used for a compound formed by other than 8–8' coupling. One of the most well-documented bioactive lignans is podophyllotoxin, from which the optimization has afforded anticancer drugs such as etoposide, teniposide, and etopophos.^{2,3} Among the neolignans, those with a dihydrobenzofuran core are worthy of particular attention for the wide range of

their biological activities, including antioxidant,⁴ antibacterial,⁵ anti-inflammatory,⁶ cardiovascular,⁷ and cytotoxic effects.^{4,8,9} Frequently cited examples are the cytotoxic¹⁰ and antiangiogenic¹¹ 3',4-di-*O*-methylcedrusin (1), the active principle of Dragon's blood (*Croton* spp.), and licarin A (2), found in the wood of *Licaria aritu* and reported as having antioxidant,¹² antiviral,¹³ cytotoxic,^{12,13} and neuroprotective activities.¹⁴ These biological reports make dihydrobenzofuran neolignans attractive targets for chemical synthesis or modification. In particular, biomimetic oxidative coupling reactions may afford “unnatural” products, maintaining a basic “natural” skeleton. Due to the lack of stereocontrol in both metal- and enzyme-mediated radical coupling, racemic mixtures are frequently obtained.¹⁵ Nevertheless, several interesting products have been obtained in such a manner, and in some cases a bioactive racemate has been resolved to obtain the more active enantiomer. A representative example is the synthetic neolignan 3, obtained by oxidative dimerization of caffeic acid methyl ester (here only the 2*R*,3*R*-enantiomer is reported), and (±)-3

Received: June 23, 2016

showed antiangiogenic¹¹ and nanomolar antiproliferative potency toward HL 60 human leukemia cells.⁸ When the enantiomers isolated were evaluated for growth inhibition of HL 60 cells, (2*R*,3*R*)-**3** showed higher inhibitory activity than (2*S*,3*S*)-**3**. Dihydrobenzofurans bearing amide functions (neolignanamides) are infrequently isolated from natural sources and include *trans*-grossamide (**4**), isolated from *Hyoscyamus niger* and other plants, which has shown anti-inflammatory¹⁶ and mild cytotoxic activity,¹⁷ and the antifungal¹⁸ and adrenergic receptor antagonist¹⁹ hordatine A (**5**), isolated initially from barley seedlings (*Hordeum vulgare*).

Given their relative rarity in Nature and the limited number of biological studies concerning these compounds, neolignanamides are worthy of deeper investigation. In addition, it is known that amides generally show a higher metabolic stability than their isosteric esters, and this may be of crucial importance if the compounds under study can be degraded by intracellular esterases before reaching their biological target. Hence, as a continuation of studies on biomimetic synthesis of lignans and neolignans with antitumor,^{20–24} antioxidant,²⁵ and antiangiogenic properties,^{26,27} we have now synthesized a small library of neolignanamides through an eco-friendly, enzyme-mediated oxidative coupling reaction. As detailed below, a preliminary screening with different oxidases indicated *Trametes versicolor* laccase as the most convenient enzyme for these syntheses. The products were purified, characterized, and evaluated for their antiproliferative activity against Caco-2 (human colon cancer cells), MCF-7 (breast adenocarcinoma cells), and PC-3 (human prostate cancer cells). The results and some structure–activity relationship considerations are reported herein.



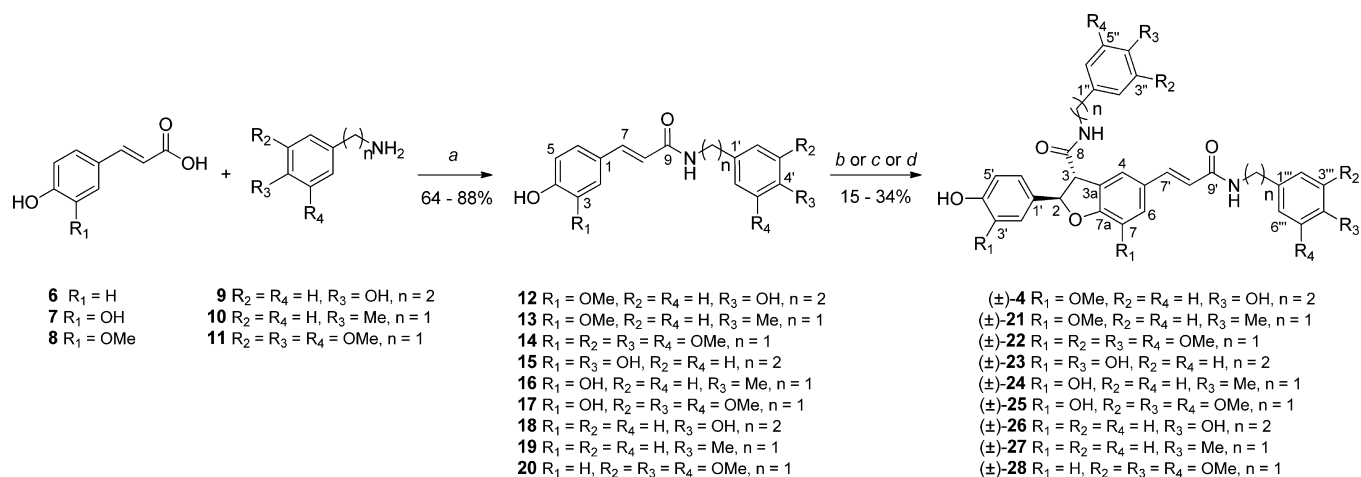
RESULTS AND DISCUSSION

A small library of new bioinspired neolignanamides was prepared by suitable monomeric amides by an amidation reaction of natural phenolic acids, namely, *p*-coumaric acid (**6**), caffeic acid (**7**), and ferulic acid (**8**). We employed three amines characterized by different steric hindrance and lipophilicity parameters, namely, 2-(4-hydroxyphenyl)ethylamine (**9**, a natural product also known as tyramine), 4-methylbenzylamine (**10**), and 3,4,5-trimethoxybenzylamine (**11**). Reactions were carried out under basic conditions (triethylamine, TEA) and in the presence of (1*H*-benzotriazol-1-yl)oxy[tris-

(dimethylamino)]phosphonium hexafluorophosphate (BOP) as a carboxyl activating agent. According to Scheme 1, nine amides (**12–20**) were synthesized, and, among these, *N*-*trans*-feruloyl tyramine (**12**), *N*-*trans*-caffeoyl tyramine (**15**), and *N*-*trans*-*p*-coumaroyl tyramine (**18**) are bioactive naturally occurring products. The other hydroxycinnamoyl amides have not been reported previously. These amides were used as substrates for a biomimetic dimerization reaction. To explore the catalytic activity of commercially available oxidases, amides **12–20** were employed in a preliminary screening on an analytical scale with three basidiomycete laccases, namely, those from *Agaricus bisporus* (AbL), *Pleurotus ostreatus* (PoL), and *Trametes versicolor* (TvL), and with horseradish peroxidase (HRP). Two sets of experiments were carried out in a biphasic system using acetate buffer (where the enzyme was solubilized), and ethyl acetate (EtOAc) or dichloromethane (CH₂Cl₂). A further set of reactions was carried out in a monophasic system consisting of 1% dimethyl sulfoxide (DMSO) in acetate buffer. The small-scale reactions were carried out at the optimal enzyme activity, namely, at 25 °C and pH 4.5.²⁸ The reactions were monitored by HPLC-UV on a C₁₈ reversed-phase silica gel column at regular time intervals in order to find the best reaction conditions. For example, the HPLC-UV profiles for the reactions of **13** in the presence of the four enzymes, employing three different cosolvents, are reported in Figure 1a–d. No products were obtained by AbL-mediated reaction even after 24 h, either for amide **13** (Figure 1a) or for the other substrates evaluated. The HRP-mediated reaction (Figure 1b) gave a low conversion of **13** into a less polar product when the reaction was carried out with EtOAc, and even less promising results were observed in CH₂Cl₂ and DMSO. Poor results were obtained using HRP also with the other substrates. The PoL-mediated reaction of **13** (Figure 1c) showed the formation of a main product, less polar than the substrate, with the conversion only partial with EtOAc and poor with the other cosolvents used. Analogous results were obtained with other amides. The best results were obtained with a TvL-mediated reaction (Figure 1d), giving almost complete conversion of **13** into a major product within 4 h, when EtOAc was used as cosolvent. Also in this case, the reactions were inferior with CH₂Cl₂ and DMSO. Analogously, the other feruloyl amides **12** and **14**, as well as compounds **18–20** (*p*-coumaroyl amides), gave a major product in the EtOAc biphasic system, whereas the caffeoyl amides **15–17** afforded a main product in the CH₂Cl₂ biphasic system.

On the basis of this preliminary screening, *Trametes versicolor* laccase was employed for preparative reactions on amides **12–20**. These afforded the natural *trans*-grossamide (**4**) and the previously unreported dimeric neolignanamides **21–28** (Scheme 1).

As detailed below, the analysis of spectroscopic data for these compounds clearly indicated the formation of dihydrobenzofuran dimers. The mechanism of formation of synthetic dihydrobenzofuran neolignans in both metal- and enzyme-mediated reactions has been previously investigated^{29,30} and is based on 8–5' radical coupling, according to Scheme 2. A reactive quinone-methide intermediate undergoes intramolecular cyclization, giving rise to the dihydrobenzofuran core. It is worth highlighting that this dimerization, even in enzyme-mediated reactions, occurs with regio- and diastereoselectivity, but not enantioselectivity,²⁹ and consequently affords *trans*-substituted racemic mixtures. In Schemes 1 and 2 only one of the two enantiomers is reported. The observed lack of

Scheme 1. Synthetic Procedure for Neolignanamides (\pm)-4 and (\pm)-21–(\pm)-28^a

^aConditions: (a) DMF, TEA, 0 °C, 15 min, BOP solution (CH₂Cl₂) 0 °C, 30 min, rt, 24 h; (b) TvL solution (acetate buffer, 0.1 M, pH = 4.7), EtOAc, 4 h, for **4**, **21**, **22**; (c) TvL solution (acetate buffer, 0.1 M, pH = 4.7), CH₂Cl₂, 2 h, for **23–25**; (d) TvL solution (acetate buffer, 0.1 M, pH = 4.7), EtOAc–DMSO, 24 h, for **26–28**. Only the 2*R*,3*R* enantiomers are reported.

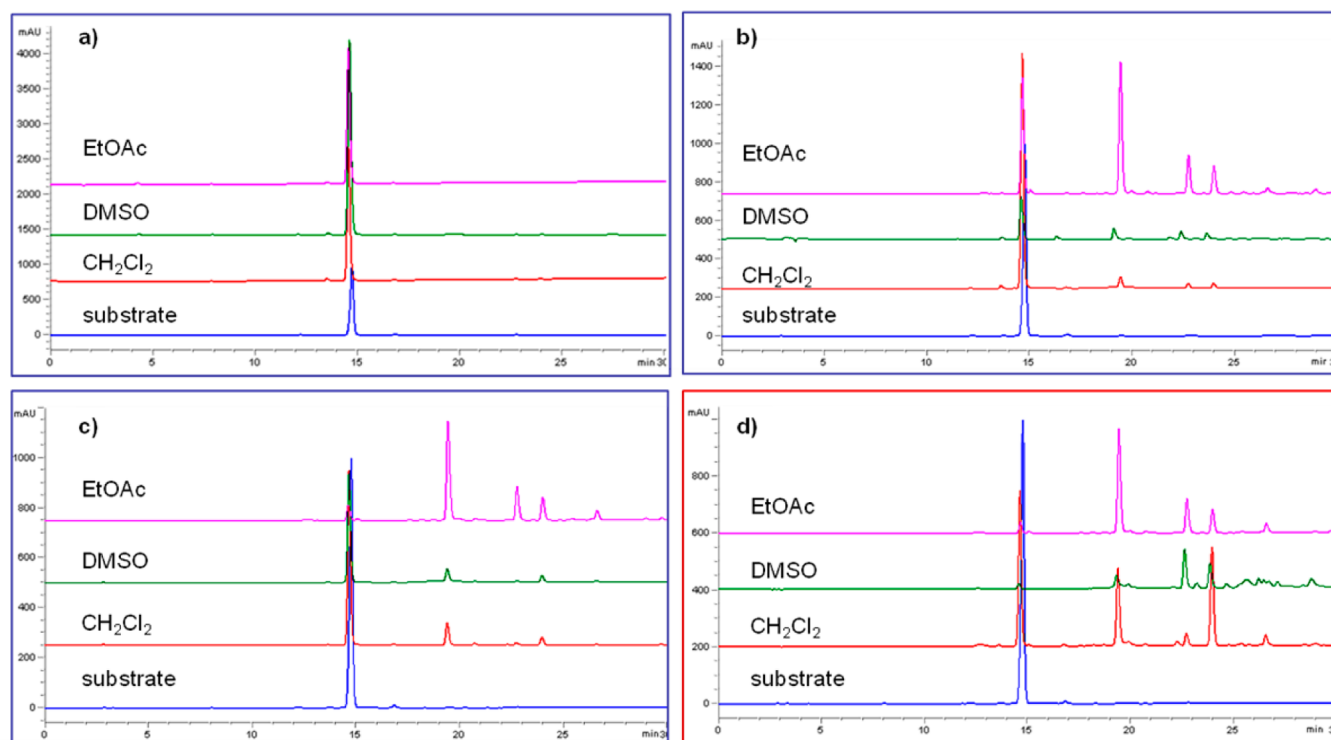


Figure 1. HPLC-UV chromatograms of **13** in the presence of (a) *Agaricus bisporus* laccase at 24 h; (b) horseradish peroxidase at 12 h; (c) *Pleurotus ostreatus* laccase at 24 h; (d) *Trametes versicolor* laccase at 4 h.

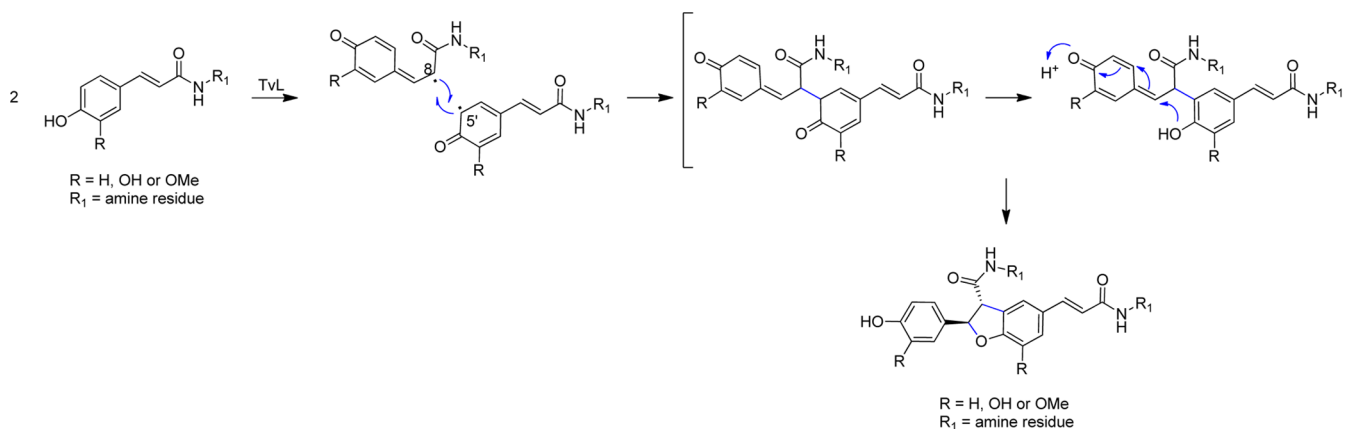
enantioselectivity in enzyme-mediated oxidative coupling reactions is not surprising when considering the known biosynthetic mechanism involving a “dirigent protein” able to control the stereochemistry of the reaction, and, in the absence of this protein, racemic mixtures are obtained.¹⁵ The observed diastereoselectivity in favor of the *trans*-substituted diastereomers is reasonably due to the lower steric hindrance in the transition state (TS) leading to the *trans* product, as supported by previous literature data for similar coupling mechanisms.^{23,31}

trans-Grossamide (**4**), bearing two tyramine pendant groups, was obtained by treating the monomeric feruloyl amide **12** with TvL in ethyl acetate–acetate buffer. The main product, isolated

by flash chromatography in 16% yield (see [Experimental Section](#) for details), was subjected to spectroscopic analysis, and the ESIMS and ¹H and ¹³C NMR data were in agreement with those previously reported³² and allowed the identification of this product as (\pm)-**4**.

The feruloyl amide **13**, treated with TvL, gave one main product. The molecular formula, C₃₆H₃₆N₂O₆, was determined by elemental analysis and ESIMS, affording a [M – H][–] peak at *m/z* 591.3. This indicated the formation of a dimeric product and was consistent with the expected structure (\pm)-**21**. The ¹H and ¹³C NMR spectra were similar to those of *trans*-grossamide, (\pm)-**4**. However, (\pm)-**21** was subjected to extensive ¹H and ¹³C

Scheme 2. Mechanism of Formation of (±)-4 and (±)-21–(±)-28



NMR analysis, including two-dimensional methods (COSY, HSQC, and HMBC), in order to establish unambiguously its structure and assign all the ^1H and ^{13}C NMR signals, as reported in Tables 1 and 2. Thus, a dihydrobenzofuran core was suggested by two mutually coupled proton signals resonating at 6.07 (H-2) and 4.34 ppm (H-3) and by the corresponding carbon signals at 88.0 (C-2) and 57.0 ppm (C-3), and this was corroborated by the key HMBC correlations of H-3, H-2', and H-6' with C-2; of H-2 and H-4 with C-3; and of H-3 and H-6 with C-7a (Figure 2). Unambiguous assignments of the resonances for the two 4-methylbenzyl pendant groups were obtained through the following HMBC correlations: from H-2, H-3, H-9 (NH), and H-10 to C-8; from H-2''/H-6'' to C-10; from H-10 and H-3''/H-5'' to C-1'; from H-2''/H-6'', H-3''/H-5'', and OCH_3 -4'' to C-4'' (C-8 pendant); from H-7', H-8', H-10' (NH), and H-11' to C-9'; from H-2'''/H-6''' to C-11'; from H-11' and H-3'''/H-5''' to C-1'''; from H-2'''/H-6''', H-3'''/H-5''', and OCH_3 -4''' to C-4''' (C-9' pendant). The *trans* relative configuration of the C-2 and C-3 substituents was established on the basis of the *J* value of 8.3 Hz for the H-2/H-3 coupling.³³ The expected *E* configuration of the C-7' and C-8' double bond was confirmed by the *J* value of 15.5 Hz for H-7'/H-8'. Thus, structure (±)-21 was established for this dimeric neolignanamide.

The feruloyl amide 14, treated as above, afforded one main product (17% yield), obtained after purification. The molecular formula was found to be $\text{C}_{40}\text{H}_{44}\text{N}_2\text{O}_{12}$, based on elemental analysis and the ESIMS spectrum ($[\text{M} - \text{H}]^-$ peak at m/z 743.3), indicating the formation of a dimer. The structure of the expected neolignanamide (±)-22, with 3,4,5-trimethoxybenzyl pendant substituents, was established on the basis of the analysis of the ^1H and ^{13}C NMR spectra as supported by two-dimensional methods, which allowed also the complete assignments of ^1H and ^{13}C NMR signals (Tables 1 and 2). The *trans* substitution at C-2, C-3 and the *E* configuration at C-7', C-8' were established as above, through coupling constant measurements.

A similar procedure was applied for the syntheses of the caffeoyl neolignan amides, employing TvL in a CH_2Cl_2 -acetate buffer biphasic solvent system. The amide 15 gave the dimer (±)-23 (15% yield) with a molecular formula of $\text{C}_{34}\text{H}_{32}\text{N}_2\text{O}_8$, based on both elemental analysis and the ESIMS ($[\text{M} - \text{H}]^-$ at m/z 595.1). Under the same conditions, 16 afforded in 16% yield the dimeric neolignanamide (±)-24, showing in its ESIMS the expected peak at m/z 563.2 ($[\text{M} - \text{H}]^-$), indicating a molecular formula of $\text{C}_{34}\text{H}_{32}\text{N}_2\text{O}_6$. The third caffeoyl amide,

17, gave a main product (24% yield), showing an ESIMS peak at m/z 715.2 ($[\text{M} - \text{H}]^-$) and with the molecular formula, $\text{C}_{38}\text{H}_{40}\text{N}_2\text{O}_{12}$, consistent with the expected structure (±)-25. In all these cases, the analyses of both ^1H and ^{13}C NMR spectra were aided by two-dimensional NMR methods, thus confirming the structures of (±)-23, (±)-24, and (±)-25 and allowing the unambiguous assignment of all NMR resonances (Tables 1 and 2).

The syntheses of the three *p*-coumaroyl neolignan amides, (±)-26–(±)-28 (with respective yields of 16%, 29%, and 34%), were carried out through TvL-mediated dimerization of amides 20–22 in the biphasic solvent system EtOAc–1% DMSO–acetate buffer. Also these products were subjected to spectroscopic characterization, in which elemental analysis and ESIMS gave the expected molecular formulas and $[\text{M} - \text{H}]^-$ peaks, respectively, at m/z 563.3 (26), 531.3 (27), and 683.4 (28). The dimeric structures were confirmed by analysis of ^1H and ^{13}C NMR spectra aided by two-dimensional experiments, thus allowing the assignments of all NMR peaks (Tables 1 and 2).

The above-mentioned racemic neolignan amides (±)-4 and (±)-21–(±)-28 were evaluated for their antiproliferative activity against three human cancer cell lines, namely, Caco-2 (human colon carcinoma), MCF-7 (human mammary adenocarcinoma), and PC-3 (human prostate cancer) cells, using 3-(4,5-dimethylthiazol-2-yl)-2,5-diphenyl tetrazolium bromide (MTT), according to the Mosmann procedure.³⁴ In Table 3, only results for compounds showing at least a GI_{50} value lower than 10 μM are included. The anticancer drug 5-fluorouracil (5-FU) was used as positive control.

Notwithstanding the close structural analogy of the compounds under study, their GI_{50} values showed a significant variation and suggested some structure–biological activity relationship information. Racemic neolignan amides bearing tyramine (4, 23, and 26) or 3,4,5-trimethoxybenzyl pendants (22, 25, and 28) were inactive or showed only moderate growth inhibition. In particular, the natural *trans*-grossamide [(±)-4] was inactive toward Caco-2 cells ($\text{GI}_{50} > 100 \mu\text{M}$) and only moderately active against MCF-7 and PC-3 cells, with GI_{50} values of 24.0 and 21.0 μM , respectively. A similar profile was observed for (±)-23, which was inactive toward Caco-2 cells and weakly active toward both PC-3 ($\text{GI}_{50} = 66.0 \mu\text{M}$) and MCF-7 cells ($\text{GI}_{50} = 39.7 \mu\text{M}$). In turn, (±)-26 was evaluated as moderately active, with GI_{50} values of 28.9 (Caco-2), 33.2 (MCF-7), and 26.0 μM (PC-3). A mild or weak activity was observed for the racemate 22 toward MCF-7 ($\text{GI}_{50} = 23.0$),

Table 1. ¹H NMR Data of Compounds (±)-21–(±)-28 (500 MHz)

position	(±)-21 ^a	(±)-22 ^a	(±)-23 ^b	(±)-24 ^a	(±)-25 ^a	(±)-26 ^a	(±)-27 ^c	(±)-28 ^c
	δ _H , mult. (J Hz)							
2	6.07, d (8.3)	6.10, d (8.3)	5.00, d (6.9)	5.18, d (6.5)	5.34, d (5.5)	6.04, d (8.0)	6.69, d (8.0)	6.75, d (8.3)
3	4.34, d (8.3)	4.35, d (8.3)	4.40, d (6.9)	4.78, d (6.5)	4.87, d (5.5)	4.14, d (8.0)	4.77, d (8.0)	4.81, d (8.3) ^d
4	7.16, s	7.13, s	6.73, s ^e	6.95, s ^f		6.84, bs	7.86, bs	7.86, s
6	7.11, s	7.06, s	6.83, s ^g	6.97, s ^f	6.97, s	7.46, dd (2.0, 8.5)	7.56, d (8.0) ^h	7.56, d (8.5) ⁱ
7						6.81, d (8.5)	7.01, d (8.0)	7.04, d (8.5)
10	4.46, t (5.0)	4.59, dd (7.0, 15.0)	3.20, m	4.37, dd (6.0, 15.0)	4.37, dd (5.7, 15.0)	3.72, m	4.83, d (6.0)	4.98, m
		4.31, dd (6.0, 15.0)	3.33, m	4.21, dd (6.0, 15.0)	4.22, dd (5.7, 15.0)	3.44, m		4.81, m
11			2.53, m			2.91–2.73, m ^l		
			2.43, m					
2'	7.02, d (2.0)	7.04, d (2.0)	7.16, d (2.0)	6.97, d (2.0) ^f	7.14, d (2.0)	7.21, d (8.5)	7.53, d (8.5) ^h	7.56, d (8.5) ⁱ
3'						6.86, d (8.5)	7.22, d (8.5)	7.22, d (8.5)
4'	OH 7.69, bs					OH 8.48, bs		
5'	6.84, d (8.0)	6.84, d (8.0)	7.10, dd (2.0, 8.4)	6.83, d (8.0)	6.95, d (8.5)	6.86, d (8.5)	7.22, d (8.5)	7.22, d (8.5)
6'	7.88, dd (2.0, 8.0)	6.89, dd (2.0, 8.0)	6.97, d (8.4)	6.76, dd (2.0, 8.0)	7.09, dd (2.0, 8.5)	7.21, d (8.5)	7.53, d (8.5) ^h	7.56, d (8.5) ⁱ
7'	7.49, d (15.5)	7.47, d (16.0)	7.43, d (15.7)	7.48, d (15.5)	7.47, d (16.0)	7.45, d (16.0)	8.13, d (15.5)	8.16, d (15.5)
8'	6.57, d (15.5)	6.38, d (16.0)	6.44, d (15.7)	6.66, d (15.5)	6.60, d (16.0)	6.48, d (16.0)	6.92, d (15.5)	6.86, d (15.5)
11'	4.47, d (5.5)	4.46, d (4.5)	3.46, t (7.4)	4.45, d (5.5)	4.43, d (5.5)	3.56, t (6.5)	4.87, dd (6.5, 13.5)	4.90, t (6.0)
12'			2.75, t (7.4)			2.91–2.73, m ^l		
2''/6''	7.22, d (8.0)	6.67, s	7.05, d (8.4)	7.04, d (8.0)	6.46, s	7.10, d (8.5)	7.44, d (7.5) ^m	6.90, s
3''/5''	7.13, d (8.0)		6.72, d (8.4) ^e	6.87, d (8.0)		6.83, d (8.5)	7.17, d (7.5) ⁿ	
4''						OH 8.79, bs		
2'''/6'''	7.24, d (8.0)	6.70, s	6.84, d (8.5) ^g	7.22, d (8.0)	6.66, s	7.10, d (8.5)	7.47, d (7.5) ^m	6.94, s
3'''/5'''	7.15, d (8.0)		6.66, d (8.5)	7.12, d (8.0)		6.78, d (8.5)	7.20, d (7.5) ⁿ	
4'''						OH 8.15, bs		
Me-4''	2.30, s			2.62, s			2.29, s	
Me-4'''	2.28, s			2.61, s			2.26, s	
OMe-7	3.90, s	3.90, s						
OMe-3'	3.81, s	3.82, s						
OMe-3''/5''		3.83, s			3.72, s			3.76, s
OMe-4''		3.72, s			3.67, s			3.93, s
OMe-3'''/5'''		3.76, s			3.79, s			3.80, s
OMe-4'''		3.68, s			3.69, s			3.97, s
NH-9	7.95, bt (5.0)			8.07, t (6.0)	7.89, t (5.7)		9.72, t (6.0)	
NH-10'	7.53, bt (5.5)	8.05, bt (4.5)		7.88, t (5.5)	7.59, t (5.5)	7.49, t (6.5)	9.11, t (6.5)	8.97, t (6.0)

^aRecorded in acetone-*d*₆. ^bRecorded in methanol-*d*₄. ^cRecorded in pyridine-*d*₅. ^{d–n}Signals with the same superscript are partially overlapped.

PC-3 cells (GI₅₀ = 38.0 μM), and Caco-2 cells (GI₅₀ = 59.1 μM), while compound (±)-25 was inactive toward all three cell lines, and (±)-28 displayed weak activity, with GI₅₀ values of 42.3 (Caco-2), 44.6 (MCF-7), and 52.0 μM (PC-3). A more effective growth inhibition was observed generally for the three neolignan amides bearing 4-methylbenzyl pendant groups: the caffeoyl dimer (±)-24, although being scarcely active toward MCF-7 cells (GI₅₀ = 42.0 μM), was more potent toward PC-3 (GI₅₀ = 12.0 μM) and Caco-2 (GI₅₀ = 16.4 μM) cells; the other dimers were potently active, with GI₅₀ values comparable or even lower than that of 5-FU (Table 3). Thus, the feruloyl dimer (±)-21 gave GI₅₀ values of 2.8 (Caco-2), 2.7 (MCF-7), and 4.8 μM (PC-3), and the *p*-coumaroyl dimer (±)-27 gave GI₅₀ values of 3.5 (Caco-2), 6.9 (MCF-7), and 3.7 μM (PC-3).

It is worthy of note that the minimal structural diversification of synthetic (±)-21 and (±)-27 with respect to the natural *trans*-grossamide, (±)-4, caused a significant enhancement of antiproliferative activity. In cell bioassays, a number of different factors may affect the results, among others cell membrane permeability, diffusion, and metabolic stability; the easily oxidizable system of caffeoyl derivatives, for instance, may affect their metabolic stability. Lipophilicity is usually a critical parameter, in particular with regard to cell uptake. Thus, to highlight a possible connection between lipophilicity and antiproliferative activity, an HPLC method was used that correlates the capacity factor (*K*) of a given compound with its lipophilicity (namely, with its log *P*).^{35–37} This method is particularly useful when the direct measurement of log *P* may

Table 2. ^{13}C NMR Data of Compounds (\pm)-21–(\pm)-28 (125 MHz)

position	(\pm)-21 ^a	(\pm)-22 ^a	(\pm)-23 ^b	(\pm)-24 ^a	(\pm)-25 ^a	(\pm)-26 ^a	(\pm)-27 ^c	(\pm)-28 ^c
	δ_{C} , type							
2	88.0, CH	88.0, CH	77.9, CH	76.9, CH	75.1, CH	87.2, CH	88.9, CH	88.4, CH
3	57.0, CH	56.8, CH	79.6, CH	78.7, CH	77.4, CH	56.3, CH	58.0, CH	57.5, CH
3a	128.4, C	128.7, C	123.1, C	127.7, C	127.7, C	127.7, C	128.4, C	127.9, C
4	111.9, CH	112.8, CH	118.5, CH	119.9, CH	119.1, CH	125.1, CH	124.6, CH	123.7, CH
5	129.0, C	129.0, C	130.6, C	130.1, C	129.3, C	127.6, C	130.0, C	128.7, C
6	116.3, CH	115.3, CH	115.6, CH	115.9, CH	114.4, CH	127.5, CH	129.9, CH	129.9, CH
7	144.5, C	144.5, C	145.0, C	146.1, C	144.8, C	109.4, CH	110.5, CH	110.1, CH
7a	149.5, C	149.4, C	145.2, C	146.8, C	145.3, C	160.6, C	161.7, C	161.3, C
8	169.5, C	169.4, C	168.8, C	166.7, C	166.3, C	169.2, C	170.9, C	170.5, C
10	42.7, CH ₂	42.98, CH ₂	42.3, CH ₂	42.7, CH ₂	42.6, CH ₂	40.4, CH ₂	43.8, CH ₂	43.8, CH ₂
11			35.5, CH ₂			33.5, CH ₂		
1'	131.6, C	131.4, C	141.2, C	144.5, C	143.4, C	131.2, C	131.5, C	128.6, C
2'	109.5, CH	109.6, CH	116.5, CH	116.2, CH	115.8, CH	115.2, CH	116.6, CH	116.2, CH
3'	147.4, C	147.5, C	146.6, C	144.4, C	143.2, C	127.2, CH	128.3, CH	128.7, CH
4'	146.6, C	146.7, C	147.3, C	144.4, C	143.2, C	157.4, C	159.4, C	159.1, C
5'	114.8, CH	114.8, CH	117.3, CH	115.2, CH	117.1, CH	127.2, CH	128.3, CH	128.7, CH
6'	118.7, CH	118.9, CH	120.6, CH	121.2, CH	121.4, CH	115.2, CH	116.6, CH	116.2, CH
7'	139.4, CH	139.6, CH	141.2, CH	139.8, CH	138.8, CH	139.9, CH	140.2, CH	139.9, CH
8'	119.3, CH	119.1, CH	118.4, CH	122.1, CH	120.3, CH	118.0, CH	120.3, CH	119.7, CH
9'	165.1, C	164.9, C	169.9, C	165.9, C	164.9, C	166.4, C	166.5, C	165.9, C
11'	42.3, CH ₂	42.93, CH ₂	42.6, CH ₂	43.1, CH ₂	42.9, CH ₂	41.0, CH ₂	43.6, CH ₂	43.8, CH ₂
12'			35.8, CH ₂			34.5, CH ₂		
1''	136.6, C	135.26, C	131.0, C	136.3, C	134.9, C	129.58, C	136.09, C	134.7, C
2''/6''	127.4, CH	104.8, CH	130.7, CH	127.8, CH	104.5, CH	129.54, CH	128.1, CH	105.1, CH
3''/5''	128.8, CH	153.23, C	116.3, CH	129.45, CH	153.2, C	115.8, CH	129.6, CH	153.7, C
4''	136.15, C	137.01, C	156.9, C	136.9, C	137.1, C	155.8, C	137.4, C	137.5, C
1'''	136.3, C	135.05, C	131.3, C	136.7, C	134.9, C	129.9, C	136.8, C	134.7, C
2'''/6'''	127.3, CH	105.0, CH	130.7, CH	128.3, CH	105.0, CH	129.4, CH	128.2, CH	105.4, CH
3'''/5'''	128.7, CH	153.33, C	116.3, CH	129.53, CH	153.3, C	115.0, CH	129.7, CH	153.7, C
4'''	136.06, C	137.26, C	156.8, C	137.4, C	137.2, C	155.6, C	137.4, C	137.7, C
Me-4''	19.9, CH ₃			20.82, CH ₃			21.06, CH ₃	
Me-4'''	19.9, CH ₃			20.83, CH ₃			21.05, CH ₃	
OMe-7	55.3, CH ₃	55.34, CH ₃						
OMe-3'	55.2, CH ₃	55.34, CH ₃						
OMe-3''/5''		55.34, CH ₃			55.27, CH ₃			55.7, CH ₃
OMe-4''		59.51, CH ₃			59.3, CH ₃			60.25, CH ₃
OMe-3'''/5'''		55.34, CH ₃			55.30, CH ₃			55.7, CH ₃
OMe-4'''		59.40, CH ₃			59.4, CH ₃			60.28, CH ₃

^aRecorded in acetone-*d*₆. ^bRecorded in methanol-*d*₄. ^cRecorded in pyridine-*d*₅.

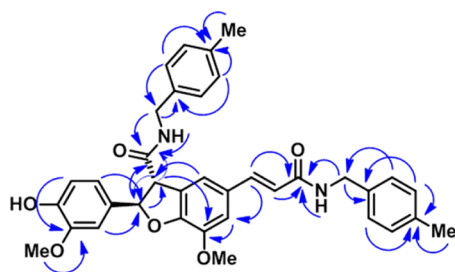


Figure 2. Key HMBC correlations (from H to C) of (\pm)-21.

be difficult for some or all compounds under study.²⁴ The HPLC profiles of neolignanamides (\pm)-4 and (\pm)-21–(\pm)-28 and that of ascorbic acid (AA), used as a highly polar reference standard, are reported in the Supporting Information. On the basis of this experimental work, the *K* values for the above-cited compounds were determined and are reported in Table 4. For

Table 3. Antiproliferative Activity of (\pm)-4 and (\pm)-21–(\pm)-28^a

compound	GI ₅₀ (μM) \pm SD ^b		
	Caco-2 ^c	MCF-7 ^d	PC-3 ^e
(\pm)-21	2.8 \pm 0.3	2.7 \pm 0.1	4.8 \pm 0.6
(\pm)-27	3.5 \pm 0.4	6.9 \pm 0.7	3.7 \pm 0.3
5-FU	4.2 \pm 0.5	3.6 \pm 0.3	6.3 \pm 1.1

^aCompounds 4, 22–26, and 28 were inactive against the tested cancer cell lines or showed GI₅₀ > 10 μM . ^bGI₅₀ calculated after 72 h of continuous exposure relative to untreated controls; values are the mean (\pm SD) of four experiments. ^cCaco-2: human colon carcinoma cells. ^dMCF-7: human mammary carcinoma cells. ^ePC-3: human prostate cancer cells.

the sake of completeness, calculated log *P* values (obtained with ACD/Labs log *P* program version 11) are added in this table.

As it is evident from these data, the neolignanamides (\pm)-21, (\pm)-24, and (\pm)-27, with the highest *K* values, also showed the

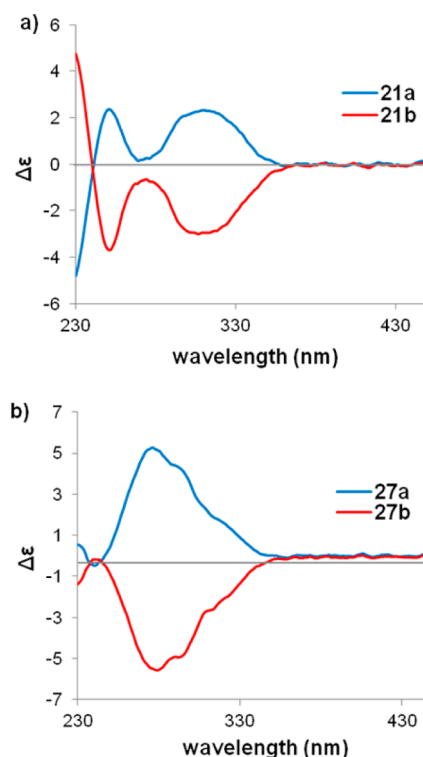
Table 4. Calculated log P and Experimental K Values of (±)-4 and (±)-21–(±)-28

compound	log P ^a	K ^b
(±)-4	2.25 ± 0.58	2.32
(±)-21	4.21 ± 0.63	8.45
(±)-22	0.50 ± 0.71	6.32
(±)-23	1.20 ± 0.58	0.56
(±)-24	3.16 ± 0.63	7.89
(±)-25	−0.55 ± 0.71	5.69
(±)-26	3.15 ± 0.49	5.20
(±)-27	5.11 ± 0.55	8.36
(±)-28	1.40 ± 0.64	6.35

^aCalculated log P values were obtained with ACD/Labs log P program version 11. ^bCapacity factors were calculated by the expression $K = (t_R - t_0)/t_0$.

highest calculated log P values and were thus the most lipophilic in this series, presumably due to the lipophilic character of the 4-methylbenzyl pendant substituents. On comparing these data with those in Table 3, it is evident that the most potent compound, (±)-21 (feruloyl dimer), is the most lipophilic, followed by the highly active compound (±)-27 (*p*-coumaroyl dimer) showing a very similar K value, with the third compound in order of lipophilicity, (±)-24 (caffeoyl dimer), also being third in order of cell growth inhibition. These data strongly suggest a possible relationship between lipophilic character (which is in turn correlated with cell membrane permeability) and antiproliferative activity. However, further structural details may play a role in interactions with the biological targets. Hence, it was decided to evaluate the possible role of the configuration at the stereogenic centers C-2 and C-3, for the most promising antiproliferative compounds (±)-21 and (±)-27. To achieve this aim, these racemic mixtures were subjected to chiral resolution to isolate the pure enantiomers. The chiral resolution of both (±)-21 and (±)-27 was carried out by HPLC on a Lux Cellulose-2 chiral column eluting with *n*-hexane–EtOH, 30:70 and 35:65, respectively (see Experimental Section). Under these conditions, the enantiomer 21a eluted with a shorter retention time (11.59 min) than enantiomer 21b (13.63 min). A similar profile was obtained for the enantiomers 27a (8.09 min) and 27b (11.42 min). To establish the absolute configuration at C-2/C-3 of the pure enantiomers, electronic circular dichroism spectroscopy (ECD) and optical rotation polarimetric measurements were employed, since comparison of ECD spectra and $[\alpha]$ values with those of closely related compounds of known absolute configuration is one of the most useful methods for this type of determination.³⁸ In particular, this approach has been applied previously to dimeric dihydrobenzofuran neolignans.^{8,19,39} The ECD spectrum of enantiomer 21a (reported in Figure 3a with a blue line) showed a positive Cotton effect in the range 250–325 nm, in agreement with the experimental $[\alpha]_D^{20}$ value of +117; conversely, the ECD spectrum of 21b (reported in Figure 3a with a red line) gave a negative Cotton effect, in agreement with the $[\alpha]_D^{20}$ value of −115. Analogously, 27a showed a positive Cotton effect (Figure 3b, blue line) and $[\alpha]_D^{20}$ value (+108), and 27b showed a negative Cotton effect (Figure 3b, red line) and $[\alpha]_D^{20}$ value (−105).

On the basis of a comparison with chiro-optical data values of closely related compounds reported in the literature, such as 1,⁴⁰ 3,⁸ (−)-ephedradine A,⁴¹ and hordatine A (5),¹⁹ the 2*S*,3*S*

**Figure 3.** ECD spectra (CH₃OH) of (a) 21a and 21b; (b) 27a and 27b.

configuration was assigned to both 21a and 27a, with the 2*R*,3*R* configuration assigned to both 21b and 27b. The pure enantiomers (2*S*,3*S*)-21, (2*R*,3*R*)-21, (2*S*,3*S*)-27, and (2*R*,3*R*)-27 were subjected to the antiproliferative activity testing toward Caco-2, MCF-7, and PC-3 cancer cells; 5-FU was used as positive reference also in this experiment. The results are summarized in Table 5 as GI₅₀ values.

Table 5. Antiproliferative Activity of (2*S*,3*S*)-21, (2*R*,3*R*)-21, (2*S*,3*S*)-27, and (2*R*,3*R*)-27

compound	GI ₅₀ (μM) ± SD ^a		
	Caco-2 ^b	MCF-7 ^c	PC-3 ^d
(2 <i>S</i> ,3 <i>S</i>)-21	1.4 ± 0.2	2.6 ± 0.1	1.6 ± 0.2
(2 <i>R</i> ,3 <i>R</i>)-21	1.1 ± 0.1	4.4 ± 0.2	2.8 ± 0.3
(2 <i>S</i> ,3 <i>S</i>)-27	3.3 ± 0.3	5.3 ± 0.1	2.5 ± 0.1
(2 <i>R</i> ,3 <i>R</i>)-27	2.1 ± 0.2	1.7 ± 0.1	2.4 ± 0.1
5-FU	3.3 ± 0.5	3.8 ± 0.4	4.1 ± 0.9

^aGI₅₀ calculated after 72 h of continuous exposure relative to untreated controls. Values are the mean (±SD) of three experiments. ^bCaco-2: human colon carcinoma. ^cMCF-7: human mammary carcinoma. ^dPC-3: human prostate cancer.

The interpretation of the data shown in Table 5 is not straightforward: both *p*-coumaroyl enantiomers resulted in comparable or higher activity than the racemic mixture, and (2*R*,3*R*)-27 was the most potent enantiomer toward all three cell lines, with GI₅₀ values of 2.1 (Caco-2 cells), 1.7 (MCF-7 cells), and 2.4 μM (PC-3 cells). The least potent enantiomer, (2*S*,3*S*)-27, was active in a micromolar range, with GI₅₀ values of 3.3, 5.3, and 2.5 μM (respectively Caco-2, MCF-7, and PC-3 cells). The feruloyl enantiomer (2*R*,3*R*)-21 was the most potent against Caco-2 cells, with a GI₅₀ value of 1.1 μM. However, the (2*S*,3*S*)-21 enantiomer was the most potent

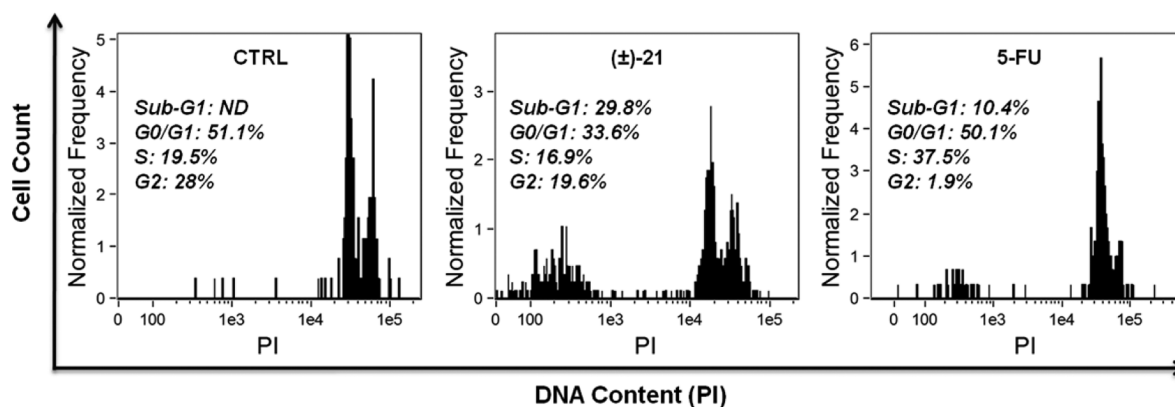


Figure 4. Cell cycle distribution of Caco-2 cells treated with compound (\pm)-21 (10 μ M, 24–36 h) and with 5-FU (100 μ M, 24–36 h) and analyzed by flow cytometry and propidium iodide staining. Data are shown as means of three independent experiments.

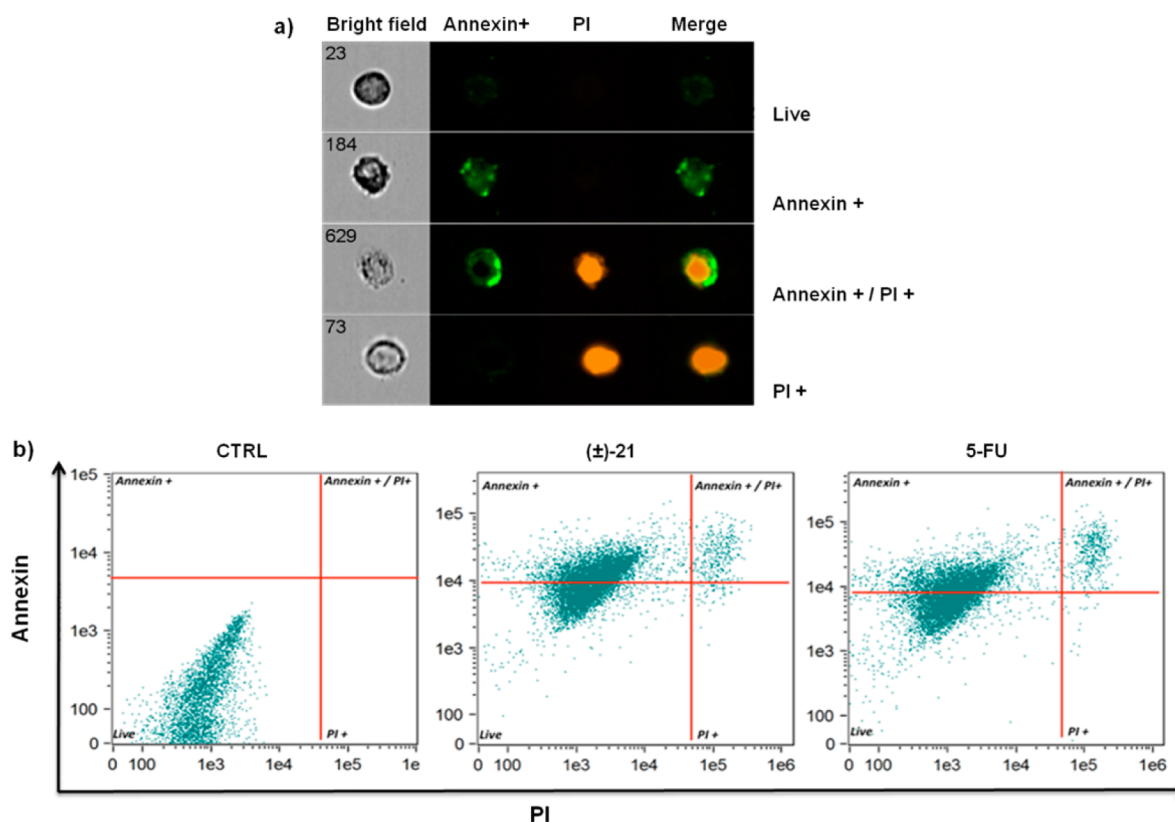


Figure 5. (a) Typical images of Caco-2 cells analyzed with a cytofluorimeter (Amnis FlowsSigh). Each cell (event) is visible in a bright field and stained by annexin-V positive, propidium iodide positive, and double positive cells. (b) Flow cytometric dot plot of specific cell populations in Caco-2 cells: live (double annexin/PI negative), early apoptosis (annexin positive), late apoptosis (double annexin/PI positive), and necrosis (annexin negative and PI positive).

against MCF-7 and PC-3 cells, showing GI_{50} values of 2.6 (MCF-7 cells) and 1.6 μ M (PC-3 cells). Both (2*S*,3*S*)-21 and (2*R*,3*R*)-21 were more potent than the racemate against Caco-2 and PC-3 cells. These data indicate that a specific configuration at C-2 and C-3 is not a structural determinant for the antiproliferative activity of these dihydrobenzofuran dimers and suggest that multiple targets (with different interactions for the 2*R*,3*R* or 2*S*,3*S* enantiomer) may be involved in their mechanism of action.

In addition, the effect of (\pm)-21 on the Caco-2 cell cycle was evaluated by flow cytometry and propidium iodide (PI) staining. Thus, Caco-2 cells were treated respectively with

compound (\pm)-21 at 10 μ M and 5-FU at 100 μ M for 24–36 h, and cell cycle changes were analyzed in comparison to vehicle-treated cells (Figure 4). Treatment with (\pm)-21 revealed the presence of cells in the sub-G1 phase (29.8%) as well as a reduction of cells in both the G0/G1 (33.6% vs 51.1%) and G2 phase (19.6% vs 28.0%). In cultures treated with 5-FU, an increase in the number of cells arrested in S phase (39.8% vs 18.0%) was observed. In addition, with respect to vehicle-treated cells, a sub-G1 phase appeared (10.4%), although of lesser intensity than that observed in cells treated with compound (\pm)-21. As is well known, 5-FU is an antimetabolite that acts by the irreversible inhibition of the enzyme

thymidylate synthetase, leading to a deficit of deoxythymidine monophosphate (dTMP) and nonfunctional DNA synthesis.⁴² Therefore, 5-FU is primarily an S phase specific drug that acts on actively proliferating cells. Cytofluorimetric data have shown that 24 h treatment with 5-FU at 100 μM produces S-phase arrest. Conversely, the inhibition of Caco-2 proliferation by compound (\pm)-21 at 10 μM could be associated with an increased DNA fragmentation, as shown by the sub-G1 peak area. It is known that DNA fragmentation is an important feature in cells undergoing apoptosis. To the best of our knowledge this is the first study to investigate the effect of neolignanamides on cell cycle progression using colorectal cancer cells.

In order to confirm if the inhibition of proliferation was due to apoptosis, cells treated with (\pm)-21 (10 μM , for 24 h) were evaluated by flow cytometry using Alexa Fluor 488 annexin V and PI (Figure 5, Table 6). The results obtained demonstrated

Table 6. (\pm)-21 Induces Apoptotic Death in Caco-2 Cells^a

Caco-2 cells	cell distribution, %		
	CTRL	(\pm)-21	5-FU
live	95.1	33.0	36.8
annexin+	3.9	58.5	56.2
annexin+/PI+	1.8	5.2	5.3
PI+	1.1	0.3	0.3

^aDetermined by Alexa Fluor 488; annexin V/propidium iodide (annexin/PI) staining after treatment with (\pm)-21 (10 μM) and 5-FU (100 μM) for 24 h. The analysis was performed on 10 000 events for each condition and expressed in percentage of total number of events.

a decreased cell viability accompanied by an increase in cells undergoing early apoptosis when compared to vehicle-treated cells. The percentage of annexin-positive cells increased from 3.9% to 58.5% in (\pm)-21-treated cells. 5-FU-treated cells were used as a positive control for apoptosis induction, resulting in strong reduction of cell viability and apoptosis induction (56.2% vs 3.9%). Under both conditions, and in vehicle-treated cells, the same low percentage of late apoptosis cells (double annexin/PI positive cells) was revealed [(\pm)-21, 5.2% vs 2.9%; 5-FU, 5.3% vs 2.9%]. In contrast, necrotic cells were not detected (PI staining alone). These data showed that (\pm)-21 exerts an antiproliferative effect by inducing cell cycle arrest and apoptosis.

In conclusion, the results of the present study have shown that bioinspired neolignanamides are worthy of further investigation to develop new potential anticancer agents, although further work will be necessary to fully delineate the underlying antitumor mechanisms.

EXPERIMENTAL SECTION

General Experimental Procedures. Optical rotations were measured with a Rudolph Research Analytical polarimeter (Autopol I, Linate, MI, Italy) at 20 °C and 589 nm. UV spectra were recorded on a PerkinElmer Lambda 25 spectrometer (Milan, Italy). ECD spectra were run on a JASCO J-810 spectropolarimeter (Cremella, LC, Italy). NMR spectra were run on a Varian Unity Inova spectrometer (Italy, Milan) operating at 499.86 (¹H) and 125.70 MHz (¹³C) and equipped with a gradient-enhanced, reverse-detection probe. Chemical shifts (δ) are indirectly referred to tetramethylsilane using residual solvent signals. The 2D g-HSQCAD experiments were performed with matched adiabatic sweeps for coherence transfer, corresponding to a central ¹³C–¹H *J* value of 146 Hz. G-HMBCAD experiments were

optimized for a long-range ¹³C–¹H coupling constant of 8.0 Hz. All NMR experiments, including 2D spectra, i.e., g-COSY, g-HSQCAD, and g-HMBCAD, were performed using software supplied by the manufacturer and acquired at constant temperature (300 K). Chloroform-*d*₁, methanol-*d*₄, acetone-*d*₆, and pyridine-*d*₅ were used as solvents. Mass spectra were acquired with an Agilent 6410 Triple Quadrupole mass spectrometer (1200 Series; Milan, Italy) equipped with a multimodal ionization source operating in MMI-ESI, in positive or negative mode. Samples infused were eluted on a cartridge (Zorbax Eclipse XDB-C18; 4.6 × 30 mm, 3.5 μm ; Agilent, Milan, Italy), with MeOH–H₂O–HCOOH (98:2:0.1) as solvent. The following parameters were used for sample ionization: gas temperature 300 °C; vaporizer temperature 250 °C; gas flow 10 L/min; nebulizer 60 psi; fragmentator 135 V; capillary voltage 3500 V; charging 2000 V. Other mass spectra were acquired with a Thermo Scientific LCQ-DECA ion trap mass spectrometer (Waltham, MA, USA) equipped with an ESI ion source operating in the negative ion mode. Samples were directly infused, and electrospray mass spectra were acquired from *m/z* 150 to 2000 using the following electrospray ion source parameters: capillary temperature 220 °C; capillary voltage –18 V; spray voltage 3.5 kV; gas flow rate 30 au. Elemental analyses were performed on a PerkinElmer 240B microanalyzer (Milan, Italy). High-performance liquid chromatography (HPLC) was carried out using an Agilent Series (Milan, Italy) G1354A pump and an Agilent UV G1315D as diode array detector. An Agilent Series 1100 G1313A autosampler was used for sample injection; an analytical reversed-phase column (Luna C₁₈, 5 μm ; 4.6 × 250 mm; Phenomenex, Castel Maggiore, BO, Italy) was employed to monitor the course of the enzymatic reactions and to determine the capacity factor value (*K*) of dihydrobenzofuran neolignanamides. Chiral resolution was carried out with HPLC on a Lux Cellulose-2 column (250 × 4.6 mm, 5 μm ; Phenomenex), and the details are reported below. Preparative liquid chromatography was performed on LiChroprep Si 60 (0.025–0.040 mm or 0.063–0.200 mm; Merck Millipore, Milan, Italy) using different solvent systems, as reported for each compound. TLC was carried out using precoated silica gel F254 plates (Merck Millipore); visualization of reaction components was achieved under UV light at wavelengths of 254 and 366 nm or by staining with a solution of cerium sulfate and phosphomolybdic acid followed by heating.

All chemicals were of reagent grade and were used without further purification. The enzymes used, namely, *Trametes versicolor* laccase (TvL, 10.0 U/mg), *Pleurotus ostreatus* laccase (PoL, 11.8 U/mg), *Agaricus bisporus* laccase (AbL, 6.8 U/mg), and horseradish peroxidase (HRP, Type I) were purchased from Sigma-Aldrich (Milan, Italy).

General Procedure for the Synthesis of Hydroxycinnamoyl Amides 12–20. Coumaric, caffeic, or ferulic acid (1 equiv) was dissolved in dry dimethylformamide (DMF) (1.0 mmol in 10.0 mL) and triethylamine (1 equiv). The solution was cooled in an ice bath for 10 min, and the suitable amine (1.3 equiv) was added; a solution of BOP in CH₂Cl₂ (1 equiv; 1 mmol in 15 mL) was added dropwise, and the mixture was stirred at 0 °C for 30 min and at room temperature for 20 h. The reaction mixture was evaporated in vacuo to remove CH₂Cl₂, the residue was partitioned between EtOAc (50 mL) and 1 N HCl solution (2 × 25 mL), and then the organic layer was partitioned with saturated NaHCO₃ solution (2 × 30 mL). The organic phase was washed with water, dried over anhydrous Na₂SO₄, filtered, and evaporated to dryness. The residue was purified by flash chromatography on silica gel and, occasionally, by further recrystallization.

N-trans-Feruloyltyramine (12). Ferulic acid (8, 201.3 mg, 1.04 mmol) was stirred with TEA (0.14 mL, 1.04 mmol) and DMF (10 mL) at 0 °C (in an ice bath) for 10 min. An excess of tyramine (9, 186.7 mg, 1.36 mmol) was added, followed by a solution of BOP in CH₂Cl₂ (459.9 mg, 1.04 mmol in 15.7 mL) gradually poured in the reaction flask. The mixture was stirred at 0 °C for 30 min and at rt overnight. After workup, the residue was purified by flash chromatography on silica gel eluting with petroleum ether–EtOAc (55:45 → 30:70), affording the amide 12 (237.6 mg, 73%): white, amorphous powder; *R*_f (TLC) 0.35 (CH₂Cl₂–MeOH, 97:3). NMR and MS spectroscopic data were in agreement with those reported in the literature.⁴³

(*E*)-*N*-(4-Methylbenzyl)-3-(4-hydroxy-3-methoxyphenyl)acrylamide (**13**). Ferulic acid (**8**, 230.2 mg, 1.18 mmol) was solubilized in dry DMF (12 mL) and kept under stirring with TEA (0.17 mL, 1.18 mmol) in an ice bath for 10 min. An excess of 4-methylbenzylamine (**10**, 0.20 mL, 1.59 mmol) was added, followed by a gradual addition of BOP (553.5 mg, 1.25 mmol, in 20 mL of CH₂Cl₂). The mixture was stirred at 0 °C for 30 min and at rt overnight. The CH₂Cl₂ was removed under vacuum, and the residue was diluted with 50 mL of EtOAc and partitioned as reported in the general procedure. The residue was purified by column chromatography on silica gel eluting with CH₂Cl₂–MeOH (100:0 → 95:5) to give **13** (287.2 mg, 82%) as a yellow oil: *R*_f (TLC) 0.37 (CH₂Cl₂–MeOH, 98:2); ¹H NMR (methanol-*d*₄, 500 MHz) δ 7.49 (1H, d, *J* = 16.0 Hz, H-7), 7.18 (2H, d, *J* = 8.5 Hz, H-3' and H-5'), 7.11* (2H, d, *J* = 8.5 Hz, H-2' and H-6'), 7.10* (1H, d, *J* = 2.0 Hz, H-2), 7.02 (1H, dd, *J* = 2.0, 8.5 Hz, H-6), 6.80 (1H, d, *J* = 8.5 Hz, H-5), 6.48 (1H, d, *J* = 16.0 Hz, H-8), 4.42 (2H, s, H-7'), 3.82 (3H, s, OCH₃), 2.26 (3H, s, CH₃), the signals with identical superscript (*) were partially overlapped; ¹³C NMR (methanol-*d*₄, 125 MHz) δ 168.9 (C, C-9), 149.8 (C, C-4), 149.2 (C, C-3), 142.3 (CH, C-7), 137.9 (C, C-4'), 136.8 (C-1'), 130.1 (CH, C-3' and C-5'), 128.6 (CH, C-2' and C-6'), 128.2 (C, C-1), 123.2 (CH, C-6), 118.7 (CH, C-8), 116.5 (CH, C-5), 111.6 (CH, C-2), 56.3 (CH₃, OCH₃-3), 44.0 (CH₂, C-7'), 21.1 (CH₃, CH₃-4'); ESIMS *m/z* 296.2 [M – H][–] (calcd for C₁₈H₁₈NO₃, 296.13); anal. C 72.68, H 6.45, N 4.70%, calcd for C₁₈H₁₉NO₃, C 72.71, H 6.44, N 4.71%.

(*E*)-*N*-(3,4,5-Trimethoxybenzyl)-3-(4-hydroxy-3-methoxyphenyl)acrylamide (**14**). Ferulic acid (**8**, 224.6 mg, 1.16 mmol) was solubilized in dry DMF (10.4 mL) and TEA (0.16 mL, 1.16 mmol), and the mixture was stirred in an ice bath for 10 min. An excess of 3,4,5-trimethoxybenzylamine (**11**, 0.18 mL, 1.30 mmol) and BOP solution (513.2 mg, 1.16 mmol, in 15.8 mL of CH₂Cl₂) were added, and the mixture was stirred at 0 °C for 30 min and at rt for 20 h. The CH₂Cl₂ was removed under vacuum, and the residue was worked up as reported in the general procedure. The crude extract was purified by flash column chromatography on silica gel using CH₂Cl₂–MeOH as eluent (99:1 → 90:10), and the product **14** was recovered (277.4 mg, 64%) as a yellow oil: *R*_f (TLC) 0.44 (petroleum ether–EtOAc, 80:20); ¹H NMR (chloroform-*d*₁, 500 MHz) δ 7.69 (1H, d, *J* = 16.0 Hz, H-7), 7.08 (1H, dd, *J* = 1.5, 8.5 Hz, H-6), 7.01 (1H, d, *J* = 1.5 Hz, H-2), 6.91 (1H, d, *J* = 8.5 Hz, H-5), 6.56 (2H, s, H-2' and H-6'), 6.28 (1H, d, *J* = 16.0 Hz, H-8), 5.84 (1H, bt, *J* = 6.5 Hz, NH), 4.51 (2H, d, *J* = 6.5 Hz, H-7'), 3.92 (6H, s, OCH₃-3' and OCH₃-5'), 3.86 (3H, s, OCH₃-3), 3.84 (3H, s, OCH₃-4'); ¹³C NMR (chloroform-*d*₁, 125 MHz) δ 165.9 (C, C-9), 153.3 (C, C-3' and C-5), 147.5 (C, C-4), 146.7 (C, C-3), 141.5 (C, C-4' and CH, C-7), 134.0 (C, C-1'), 127.3 (C, C-1), 122.2 (CH, C-6), 117.9 (CH, C-8), 114.7 (CH, C-5), 109.6 (CH, C-2), 105.1 (CH, C-2' and C-6'), 60.9 (CH₃, OCH₃-4'), 56.2 (CH₃, OCH₃-3' and OCH₃-5'), 55.9 (CH₃, OCH₃-3), 44.2 (CH₂, C-7'); ESIMS *m/z* 372.1 [M – H][–] (calcd for C₂₀H₂₂NO₆, 372.14); anal. C 64.31, H 6.18, N 3.77%, calcd for C₂₀H₂₃NO₆, C 64.33, H 6.21, N 3.75%.

N-trans-Caffeoyltyramine (**15**). Caffeic acid (**7**, 310.2 mg, 1.72 mmol) was stirred with TEA (0.24 mL, 1.73 mmol) in dry DMF (17.5 mL) in an ice bath for 10 min. Then, tyramine (**9**, 306.3 mg, 2.23 mmol) and gradually the BOP solution (760.2 mg, 1.72 mmol in 25.4 mL of CH₂Cl₂) were added. The mixture was stirred at 0 °C for 30 min and then at rt overnight. The reaction was quenched by partition as described above. The dried organic phase was evaporated in vacuo and chromatographed on silica gel eluting with CHCl₃–MeOH (98:2 → 85:15); the amide **15** was obtained after crystallization in CH₂Cl₂–MeOH (396.1 mg, yield: 77%): yellow, amorphous powder; *R*_f (TLC) 0.37 (CHCl₃–MeOH, 92:8). The acquired MS and NMR data are in agreement with those previously reported.⁴⁴

(*E*)-*N*-(4-Methylbenzyl)-3-(3,4-dihydroxyphenyl)acrylamide (**16**). Caffeic acid (**7**, 358.7 mg, 1.98 mmol) was dissolved in dry DMF (20.0 mL), and the solution was stirred with TEA (0.28 mL, 1.99 mmol) at 0 °C. After 10 min, amine **10** (0.25 mL, 1.98 mmol) and BOP solution (876.9 mg, 1.98 mmol, in 30.2 mL of CH₂Cl₂) were added dropwise to the mixture. The reaction was stirred at 0 °C for 30 min and at rt overnight. The CH₂Cl₂ was removed by evaporation, and

the residue was partitioned using EtOAc (100 mL) as reported in the general procedure. The crude mixture was purified by a flash chromatography column on silica gel eluting with petroleum ether–EtOAc (60:40 → 30:70), and the amide **16** (364.7 mg, 65%) was recovered as a yellow powder: *R*_f (TLC) 0.50 (petroleum ether–EtOAc, 30:70); ¹H NMR (methanol-*d*₄, 500 MHz) δ 7.43 (1H, d, *J* = 15.5 Hz, H-7), 7.19 (2H, d, *J* = 8.0 Hz, H-3' and H-5'), 7.14 (2H, d, *J* = 8.0 Hz, H-2' and H-6'), 7.01 (1H, d, *J* = 2.0 Hz, H-2), 6.91 (1H, dd, *J* = 2.0, 9.0 Hz, H-6), 6.76 (1H, d, *J* = 9.0 Hz, H-5), 6.40 (1H, d, *J* = 15.5 Hz, H-8), 4.42 (2H, s, H-7'), 2.31 (3H, s, CH₃); ¹³C NMR (methanol-*d*₄, 125 MHz) δ 167.7 (C, C-9), 147.4 (C, C-4), 145.3 (C, C-3), 141.0 (CH, C-7), 136.5 (C, C-4'), 135.5 (C-1'), 128.7 (CH, C-3' and C-5'), 127.2 (C, C-1 and CH, C-2' and C-6'), 126.9 (CH, C-6), 120.7 (CH, C-8), 115.0 (CH, C-5), 113.7 (CH, C-2), 42.6 (CH₂, C-7'), 19.7 (CH₃, CH₃-4'); ESIMS *m/z* 282.1 [M – H][–] (calcd for C₁₇H₁₆NO₃, 282.11); anal. C 72.05, H 6.07, N 4.91%, calcd for C₁₇H₁₇NO₃, C 72.07, H 6.05, N 4.94%.

(*E*)-*N*-(3,4,5-Trimethoxybenzyl)-3-(3,4-dihydroxyphenyl)acrylamide (**17**). Caffeic acid (**7**, 302.4 mg, 1.68 mmol) and TEA (0.24 mL, 1.69 mmol) were stirred in dry DMF (15.4 mL) at 0 °C for 10 min. Then, 3,4,5-trimethoxybenzylamine (**11**, 0.35 mL, 2.21 mmol) and gradually the BOP solution (752.4 mg; 1.68 mmol; in 30.5 mL of CH₂Cl₂) were poured in the mixture. The reaction was stirred at 0 °C for 30 min and at rt for 24 h. The CH₂Cl₂ was evaporated, and the residue was diluted with 80 mL of EtOAc and partitioned as reported in the general procedure. Flash column chromatography on silica gel eluted with CHCl₃–MeOH (99:1 → 90:10) gave amide **17** (385.9 mg, 64%) as a yellow, amorphous powder: *R*_f (TLC) 0.22 (CHCl₃–MeOH, 93:7); ¹H NMR (methanol-*d*₄, 500 MHz) δ 7.44 (1H, d, *J* = 15.0 Hz, H-7), 7.01 (1H, d, *J* = 2.0 Hz, H-2), 6.91 (1H, dd, *J* = 2.0, 8.5 Hz, H-6), 6.76 (1H, d, *J* = 8.5 Hz, H-5), 6.42 (1H, d, *J* = 15.0 Hz, H-8), 6.64 (2H, s, H-2' and H-6'), 4.42 (2H, s, H-7'), 3.82 (6H, s, OCH₃-3' and OCH₃-5'), 3.74 (3H, s, OCH₃-4'); ¹³C NMR (methanol-*d*₄, 125 MHz) δ 169.2 (C, C-9), 154.6 (C, C-3' and C-5'), 148.9 (C, C-4), 146.7 (C, C-3), 142.7 (CH, C-7), 138.2 (C, C-4'), 136.2 (C-1'), 128.2 (C, C-1), 122.3 (CH, C-6), 118.2 (CH, C-8), 116.5 (CH, C-5), 115.1 (CH, C-2), 106.0 (CH, C-2' and C-6'), 61.1 (CH₃, OCH₃-4'), 56.6 (CH₃, OCH₃-3' and OCH₃-5'), 44.5 (CH₂, C-7'); ESIMS *m/z* 358.1 [M – H][–] (calcd for C₁₉H₂₀NO₆, 358.13); anal. C 63.56, H 5.88, N 3.92%, calcd for C₁₉H₂₁NO₆, C 63.50, H 5.89, N 3.90%.

N-trans-*p*-Coumaroyltyramine (**18**). Coumaric acid (**6**, 478.5 mg, 2.91 mmol) was solubilized in dry DMF (25.0 mL), and the solution was stirred with TEA (0.40 mL, 2.90 mmol) at 0 °C for 10 min. Tyramine (**9**, 558.3 mg, 3.78 mmol) was added to the mixture, and subsequently a solution of BOP (1286.2 mg, 2.91 mmol, in 50 mL of CH₂Cl₂) was added dropwise. The mixture was stirred at 0 °C for 30 min and at rt overnight. The CH₂Cl₂ was removed by evaporation, and the residue diluted with EtOAc (140 mL) was extracted as described above. The crude mixture was purified by flash chromatography on silica gel eluting with CHCl₃–MeOH (98:2 → 80:20), and the amide **18** (616.8 mg, 75%) was recovered as a white, amorphous powder: *R*_f (TLC) 0.36 (CHCl₃–MeOH, 92:8); NMR and MS data were in agreement with values reported in the literature.⁴³

(*E*)-*N*-(4-Methylbenzyl)-3-(4-hydroxyphenyl)acrylamide (**19**). Coumaric acid (**6**, 225.1 mg, 1.37 mmol) was stirred with TEA (0.19 mL, 1.37 mmol) in dry DMF (14.2 mL) at 0 °C for 10 min. Then, an excess of 4-methylbenzylamine (**10**, 0.24 mL, 1.78 mmol) was added, and a solution of BOP in CH₂Cl₂ (685.1 mg, 1.54 mmol, 23.2 mL) was added dropwise. The mixture was stirred at 0 °C for 30 min and at rt overnight. The reaction mixture was evaporated under vacuum to remove CH₂Cl₂, and the residue was partitioned as reported in the general procedure. Purification by silica gel column chromatography with CHCl₃–MeOH (100:0 → 95:5) gave the pure amide **19** (322.4 mg, 88%) as a white, amorphous powder: *R*_f (TLC) 0.44 (CH₂Cl₂–MeOH, 93:7); ¹H NMR (methanol-*d*₄, 500 MHz) δ 7.49 (1H, d, *J* = 15.7 Hz, H-7), 7.41 (2H, d, *J* = 8.5 Hz, H-2 and H-6), 7.20 (2H, d, *J* = 8.0 Hz, H-3' and H-5'), 7.14 (2H, d, *J* = 8.0 Hz, H-2' and H-6'), 6.79 (2H, d, *J* = 8.5 Hz, H-3 and H-5), 6.45 (1H, d, *J* = 15.7 Hz, H-8), 4.43 (2H, s, H-7'), 2.31 (3H, s, CH₃-4'); ¹³C NMR

(methanol- d_4 , 125 MHz) δ 169.1 (C, C-9), 160.5 (C, C-4), 142.1 (CH, C-7), 138.0 (C, C-4'), 136.9 (C-1'), 130.6 (CH, C-2 and C-6), 130.1 (CH, C-3' and C-5'), 128.6 (C-2' and C-6'), 127.7 (C, C-1), 118.3 (CH, C-8), 116.7 (CH, C-3 and C-5), 44.1 (CH₂, C-7'), 21.1 (CH₃, CH₃-4'); ESIMS m/z 266.1 [M - H]⁻ (calcd for C₁₇H₁₆NO₂, 266.12); anal. C 76.35, H 6.43, N 5.26%, calcd for C₁₇H₁₇NO₂, C 76.38, H 6.41, N 5.24%.

(*E*)-*N*-(3,4,5-Trimethoxybenzyl)-3-(4-hydroxyphenyl)acrylamide (**20**). Coumaric acid (**6**, 449.0 mg, 2.73 mmol) was dissolved in dry DMF (28 mL) and TEA (0.38 mL, 2.73 mmol). The mixture was stirred in an ice bath for 10 min, and subsequently, the amine **11** (0.60 mL, 3.55 mmol) and gradually the BOP solution (1420.6 mg; 3.21 mmol in 42.4 mL of CH₂Cl₂) were added. The mixture was stirred at 0 °C for 30 min and then at rt overnight. The mixture was concentrated by evaporation and partitioned as described in the general procedure. The flash chromatography column with silica gel, eluted with petroleum ether–EtOAc (85:15 → 20:80), afforded the amide **20**, after crystallization in CH₂Cl₂–MeOH (615 mg, 67%), as a white, amorphous powder: R_f (TLC) 0.41 (CH₂Cl₂–MeOH, 98:2); ¹H NMR (methanol- d_4 , 500 MHz) δ 7.55 (1H, d, J = 15.5 Hz, H-7), 7.41 (2H, d, J = 8.5 Hz, H-2 and H-6), 6.79 (2H, d, J = 8.5 Hz, H-3 and H-5), 6.64 (2H, s, H-2' and H-6'), 6.46 (1H, d, J = 15.7 Hz, H-8), 4.42 (2H, s, H-7'), 3.82 (6H, s, OCH₃-3' and OCH₃-5'), 3.74 (3H, s, OCH₃-4'); ¹³C NMR (methanol- d_4 , 125 MHz) δ 169.1 (C, C-9), 160.6 (C, C-4), 154.6 (C, C-3' and C-5'), 142.3 (CH, C-7), 138.3 (C, C-4'), 136.2 (C-1'), 130.6 (CH, C-2 and C-6), 127.7 (C, C-1), 118.2 (CH, C-8), 116.7 (CH, C-3 and C-5), 106.0 (C-2' and C-6'), 61.1 (CH₃, OCH₃-4'), 56.6 (CH₃, OCH₃-3' and OCH₃-5'), 44.5 (CH₂, C-7'); ESIMS m/z 342.2 [M - H]⁻ (calcd for C₁₉H₂₀NO₅, 342.13); anal. C 66.42, H 6.18, N 4.05%, calcd for C₁₉H₂₁NO₅, C 66.46, H 6.16, N 4.08%.

Biomimetic Synthesis of Dihydrobenzofuran Neolignan-amides (±)-4 and (±)-21–(±)-28. Preliminary Screening. Aliquots (2.0 mg) of the amides **12–20** were dissolved in three different solvents (1 mL), namely, EtOAc, CH₂Cl₂, and 2% DMSO in acetate buffer (0.1 M pH = 4.5). The three different solutions of each compound were treated with the following enzymes: TvL, PoL, Abl, and HRP (2 mg), previously dissolved in acetate buffer (1.0 mL, 0.1M, pH = 4.5). The reactions were stirred at rt in vials without caps except for HRP-mediated reactions; in the latter, a 30% (v/v) H₂O₂ solution (1.0 μ L) was added to each mixture, and the reactions were carried out in capped vials. For each experiment, a blank was carried out in the same conditions, without enzyme. The reactions were monitored at regular time intervals by HPLC with a reversed-phase column (RP-18) with the following gradient of CH₃CN/H⁺ (99:1 v/v; B) in H₂O/H⁺ (99:1 v/v; A) at 1 mL/min: $t_{0 \text{ min}}$ B = 30%, $t_{30 \text{ min}}$ B = 80%. A diode array detector was set at 254, 280, 305, and 325 nm.

Trametes versicolor laccase gave the best results in terms of both substrate conversion and formation of a main product, and it was employed to obtain the dimers on a preparative scale.

(±)-*trans*-Grossamide (**4**). Feruloyl amide **12** (120.3 mg, 0.38 mmol) was dissolved in EtOAc (60.0 mL), and the organic solution was stirred with acetate buffer solution containing the enzyme TvL (115.8 mg dissolved in 58.0 mL). The reaction was carried out at rt for 4 h. The reaction was quenched by phase separation, and the aqueous phase was partitioned with EtOAc (2 × 25 mL). The combined organic phases were washed with water, dried over anhydrous Na₂SO₄, and filtered, and then the solvent was evaporated. Purification by flash column chromatography on silica gel with CHCl₃–MeOH (98:2 → 90:10) afforded the dihydrobenzofuran (±)-**4** as a racemic mixture of *trans*-diastereomers (19.3 mg, 16%), as a yellow oil: R_f (TLC) 0.29 (CHCl₃–MeOH, 90:10); the spectroscopic data were in agreement with previous values reported in the literature.³²

2-(4-Hydroxy-3-methoxyphenyl)-7-methoxy-N-(4-methylbenzyl)-5-[(*E*)-3-(4-methylbenzyl)amino-3-oxoprop-1-en-1-yl]-2,3-dihydrobenzofuran-3-carboxamide [(±)-**21**]. Amide **13** (122.6 mg, 0.41 mmol) was solubilized in EtOAc (61.3 mL), and the organic solution was stirred with the enzyme solution (118.2 mg of TvL in 59.1 mL of acetate buffer) at rt for 4 h. The two phases were separated, and the aqueous phase was partitioned with EtOAc (2 × 25 mL). The total

organic phase was finally washed with water, dried, and evaporated in vacuo. Flash chromatography with silica gel, eluted with petroleum ether–EtOAc (65:35 → 25:75%), gave the racemate neolignanamide (±)-**21** (19.3 mg, 16%) as a white, amorphous powder: R_f (TLC) 0.46 (CH₂Cl₂–MeOH, 93:7); UV (MeOH) λ_{max} (log ϵ) 290 (4.49), 304 (4.51), 321 (4.56) nm; ¹H and ¹³C NMR data, see Tables 1 and 2; ESIMS m/z 591.3 [M - H]⁻ (calcd for C₃₆H₃₅N₂O₆, 591.25); anal. C 72.93, H 6.13, N 4.75%, calcd for C₃₆H₃₆N₂O₆, C 72.95, H 6.12, N 4.73%.

2-(4-Hydroxy-3-methoxyphenyl)-7-methoxy-5-[(*E*)-3-oxo-3-(3,4,5-trimethoxybenzyl)aminoprop-1-en-1-yl]-N-(3,4,5-trimethoxybenzyl)-2,3-dihydrobenzofuran-3-carboxamide [(±)-**22**]. Compound **14** (74.6 mg, 0.20 mmol) was dissolved in EtOAc (37.3 mL), and a solution containing TvL (85.0 mg in 42.5 mL of acetate buffer 0.1 M, pH = 4.5) was added. The resulting biphasic system was stirred at rt for 4 h. The crude mixture was quenched by phase separation, and the aqueous layer was partitioned with EtOAc (2 × 15 mL). The organic residue was purified by a flash chromatography column on silica gel eluting with CH₂Cl₂–MeOH (99:1 → 90:10), affording the racemate (±)-**22** (12.5 mg, 17%) as a yellow oil: R_f (TLC) 0.16 (CH₂Cl₂–MeOH, 95:5); ¹H and ¹³C NMR data, see Tables 1 and 2; ESIMS m/z 743.3 [M - H]⁻ (calcd for C₄₀H₄₃N₂O₁₂, 743.28); anal. C 64.48, H 5.97, N 3.73%, calcd for C₄₀H₄₄N₂O₁₂, C 64.51, H 5.95, N 3.76%.

2-(3,4-Dihydroxyphenyl)-7-hydroxy-N-(4-hydroxyphenethyl)-5-[(*E*)-3-(4-hydroxyphenethyl)amino-3-oxoprop-1-en-1-yl]-2,3-dihydrobenzofuran-3-carboxamide [(±)-**23**]. Caffeoyl amide **15** (118.2 mg, 0.40 mmol) was dissolved in CH₂Cl₂ (59.2 mL), and the mixture was stirred with a solution of TvL (108.6 mg in 54.3 mL of 0.1 M acetate buffer, pH = 4.5) at rt for 2 h. The reaction was quenched by phase separation, and the aqueous phase was partitioned with CH₂Cl₂ (2 × 25 mL). The combined organic phases were washed with water, dried over anhydrous Na₂SO₄, filtered, and taken to dryness. The silica gel column chromatography eluted with CHCl₃–MeOH (97:3 → 85:15) afforded the racemate (±)-**23** (18.2 mg, 15%) as a yellow oil: R_f (TLC) 0.41 (CHCl₃–MeOH, 88:12); UV (MeOH) λ_{max} (log ϵ) 285 (4.05), 320 (3.93) nm; ¹H and ¹³C NMR data, see Tables 1 and 2; ESIMS m/z 595.1 [M - H]⁻ (calcd for C₃₄H₃₁N₂O₈, 595.21); anal. C 68.41, H 5.43, N 4.69%, calcd for C₃₄H₃₂N₂O₈, C 68.45, H 5.41, N 4.70%.

2-(3,4-Dihydroxyphenyl)-7-hydroxy-N-(4-methylbenzyl)-5-[(*E*)-3-(4-methylbenzyl)amino-3-oxoprop-1-en-1-yl]-2,3-dihydrobenzofuran-3-carboxamide [(±)-**24**]. The amide **16** (131.2 mg, 0.46 mmol) was dissolved in CH₂Cl₂ (65.6 mL), and a TvL solution in acetate buffer (128.4 mg of 64.8 mL) was added. The reaction was stirred at rt for 2 h. After the two phases were separated, the aqueous phase was partitioned with CH₂Cl₂ (2 × 25 mL), and finally the combined organic phases were washed with water, dried, and evaporated to dryness. Flash chromatography on silica gel, eluted with CH₂Cl₂–MeOH (98:2 → 95:5), afforded the racemic dimer (±)-**24** (21.2 mg, 16%) as a yellow oil: R_f (TLC) 0.56 (CH₂Cl₂–MeOH, 92:8); UV (MeOH) λ_{max} (log ϵ) 240 (4.60), 282 (4.66), 318 (4.36) nm; ¹H and ¹³C NMR data, see Tables 1 and 2; ESIMS m/z 563.2 [M - H]⁻ (calcd for C₃₄H₃₁N₂O₆, 563.22); anal. C 72.29, H 5.68, N 4.95%, calcd for C₃₄H₃₂N₂O₆, C 72.32, H 5.71, N 4.96%.

2-(3,4-Dihydroxyphenyl)-7-hydroxy-5-[(*E*)-3-oxo-3-(3,4,5-trimethoxybenzyl)aminoprop-1-en-1-yl]-N-(3,4,5-trimethoxybenzyl)-2,3-dihydrobenzofuran-3-carboxamide [(±)-**25**]. The amide **17** (105.8 mg, 0.29 mmol) was solubilized in CH₂Cl₂ (53.0 mL). The mixture was stirred with a TvL solution previously prepared (104.2 mg, in 52.2 mL of acetate buffer, pH = 4.5) at rt for 2 h. The reaction was quenched by separation of the two phases, with the aqueous phase partitioned with EtOAc (2 × 25 mL), and the total organic phase was washed with water, dried over Na₂SO₄, filtered, and evaporated to dryness. The crude mixture was purified by silica gel flash chromatography eluted with CHCl₃–MeOH (100:0 → 90:10), giving the neolignanamide (±)-**25** (24.8 mg, 24%) as a yellow oil: R_f (TLC) 0.55 (CHCl₃–MeOH, 92:8); UV (MeOH) λ_{max} (log ϵ) 284 (4.44), 316 (4.26) nm; ¹H and ¹³C NMR data, see Tables 1 and 2; ESIMS m/z 715.2 [M - H]⁻ (calcd for C₃₈H₃₉N₂O₁₂, 715.25); anal. C 63.65, H 5.60, N 3.87%, calcd for C₃₈H₄₀N₂O₁₂, C 63.68, H 5.63, N 3.91%.

N-(4-Hydroxyphenethyl)-5-[(*E*)-3-(4-hydroxyphenethyl)amino-3-oxoprop-1-en-1-yl]-2-(4-hydroxyphenyl)-2,3-dihydrobenzofuran-3-carboxamide [(±)-26]. Coumaroyl amide **18** (105.3 mg, 0.37 mmol) was dissolved in DMSO–EtOAc (1:99; 51.0 mL). The mixture was stirred with a solution of TvL (102.0 mg in 51.3 mL of acetate buffer) at rt for 24 h. The two phases were separated, the aqueous layer was partitioned with EtOAc (2 × 20 mL), and the combined organic phases were washed with water, dried, and evaporated. Purification by flash column chromatography on silica gel, eluted with CH₂Cl₂–MeOH (98:2 → 90:10), afforded the racemate (±)-**26** (16.8 mg, 16%) as a white, amorphous powder: *R_f* (TLC) 0.35 (CH₂Cl₂–MeOH, 92:8); UV (MeOH) λ_{max} (log ε) 286 (4.42), 313 (4.38) nm; ¹H and ¹³C NMR data, see Tables 1 and 2; ESIMS *m/z* 563.3 [M – H][–] (calcd for C₃₄H₃₁N₂O₆, 563.22); anal. C 72.27, H 5.75, N 4.93%, calcd for C₃₄H₃₂N₂O₆, C 72.32, H 5.71, N 4.96%.

2-(4-Hydroxyphenyl)-*N*-(4-methylbenzyl)-5-[(*E*)-3-(4-methylbenzyl)amino-3-oxoprop-1-en-1-yl]-2,3-dihydrobenzofuran-3-carboxamide [(±)-27]. Amide **19** (130.8 mg, 0.49 mmol) was dissolved in DMSO–EtOAc (1:99; 65.1 mL), and the mixture was stirred with TvL solution (115.2 mg in 57.8 mL of acetate buffer) at rt for 24 h. After the separation of the two phases, the aqueous layer was partitioned with EtOAc (2 × 25 mL) and the total organic phase was washed with water, dried over anhydrous Na₂SO₄, filtered, and evaporated in vacuo. The crude mixture was purified by flash column chromatography on silica gel with CH₂Cl₂–MeOH (100:0 → 95:5), and the neolignanamide (±)-**27** was obtained after crystallization (acetone; 38.3 mg, 29%) as a white, amorphous powder: *R_f* (TLC) 0.25 (CH₂Cl₂–MeOH, 96:4); UV (MeOH) λ_{max} (log ε) 297 (4.11), 310 (4.09) nm; ¹H and ¹³C NMR data, see Tables 1 and 2; ESIMS *m/z* 531.3 [M – H][–] (calcd for C₃₄H₃₁N₂O₄, 531.23); anal. C 76.64, H 6.03, N 5.28%, calcd for C₃₄H₃₂N₂O₄, C 76.67, H 6.06, N 5.26%.

2-(4-Hydroxyphenyl)-5-[(*E*)-3-oxo-3-(3,4,5-trimethoxybenzyl)aminoprop-1-en-1-yl]-*N*-(3,4,5-trimethoxybenzyl)-2,3-dihydrobenzofuran-3-carboxamide [(±)-28]. Coumaroyl amide **20** (117.6 mg, 0.34 mmol) was solubilized in DMSO–EtOAc (1:99; 58.6 mL), and this solution was stirred together with the enzyme solution (108.2 mg of TvL in 54.5 mL of acetate buffer, pH = 4.5) at rt for 24 h. After separation, the aqueous layer was partitioned with EtOAc (2 × 25 mL), and the combined organic layers were washed with water, dried, and evaporated in vacuo. Silica gel column chromatography, eluted with CH₂Cl₂–acetone (96:4 → 80:20), gave the dimer (±)-**28** (39.4 mg, 34%) as a white, amorphous powder: *R_f* (TLC) 0.35 (CH₂Cl₂–acetone, 84:16); UV (MeOH) λ_{max} (log ε) 276 (4.59), 322 (4.21) nm; ¹H and ¹³C NMR data, see Tables 1 and 2; ESIMS *m/z* 683.4 [M – H][–] (calcd for C₃₈H₃₉N₂O₁₀, 683.26); anal. C 66.61, H 5.92, N 4.04%, calcd for C₃₈H₄₀N₂O₁₀, C 66.65, H 5.89, N 4.09%.

Measurement of the Capacity Factor (*K*). Measurements of the capacity factor of neolignanamides (±)-**4** and (±)-**21**–(±)-**28** were performed using a Luna-C₁₈ column, and as eluent a gradient of H₂O/H⁺ (99/1; A)–CH₃CN/H⁺ (99/1; B) was used at 1 mL/min with the following eluting profile: *t*_{0 min} B = 20%, *t*_{30 min} B = 80%. The capacity factor *K* was calculated using the following expression: $K = (t_R - t_0)/t_0$, where *t_R* is the retention time of the test substance and *t₀* is the retention time of AA used as standard. Calculated log *P* values were obtained with the ACD/Labs log *P* program version 11.

Chiral Resolution of Racemic Mixtures (±)-21** and (±)-**27**.** Racemic neolignanamide **21** (5.7 mg) was dissolved in EtOH (1.5 mL) and resolved by HPLC–UV using a Lux Cellulose-2 chiral column (eluting solvent: *n*-hexane–EtOH, 30:70; flow rate 0.5 mL/min; 30 injections; 50 μL each) to yield two enantiomers. Enantiomer **21a** (2.5 mg): (2*S*,3*S*)-**21**; white, amorphous powder; *t_R* 11.59 min; [α]_D²⁰ +117 (c 0.1, CH₃OH); ECD (MeOH) λ_{max} (Δε) 250 (+2.36), 310 (+2.32) nm. Enantiomer **21b** (2.6 mg): (2*R*,3*R*)-**21**; white, amorphous powder; *t_R* 13.63 min; [α]_D²⁰ –115 (c 0.1, CH₃OH); ECD (MeOH) λ_{max} (Δε) 250 (–3.69), 310 (–2.96) nm.

Racemic neolignanamide **27** (6.1 mg) was dissolved in EtOH (1.5 mL) and was resolved by HPLC–UV using a Lux Cellulose-2 chiral column (eluting solvent: *n*-hexane–EtOH, 35:65; flow rate 0.5 mL/min; 30 injections; 50 μL each) to yield two enantiomers. Enantiomer **27a** (2.8 mg): (2*S*,3*S*)-**27**; white, amorphous powder; *t_R* = 8.09 min;

[α]_D²⁰ +108 (c 0.1, CH₃OH); ECD (MeOH) λ_{max} (Δε) 276 (+5.25), 292 (+4.32). Enantiomer **27b** (2.7 mg): (2*R*,3*R*)-**27**; white, amorphous powder; *t_R* = 11.42 min; [α]_D²⁰ –105 (c 0.1, CH₃OH); ECD (MeOH) λ_{max} (Δε) 276 (–5.88), 292 (–4.95) nm.

Antiproliferative Activity Assay. Human Cell Cultures. Human colorectal adenocarcinoma cell line Caco-2 (ATCC number: HTB-37), human mammary adenocarcinoma MCF-7 (ATCC number: HTB22), and human prostate cancer PC-3 (ATCC number: CLR-1435) have been used in the present work and have been cultured as previously reported.⁴⁵

Treatment with Neolignanamides (±)-4** and (±)-**21**–(±)-**28** and MTT Colorimetric Assay.** Human cancer cell lines ((2.5–3.0) × 10⁵ cells/0.33 cm²) were plated in Nunclon Microwell (Nunc) 96-well plates and were incubated at 37 °C. After 24 h, cells were treated with the compounds under study (final concentration 0.01–100 μM). Cells treated with 0.5–1% DMSO were used as controls. Microplates were incubated at 37 °C in a humidified atmosphere of 5% CO₂ and 95% air for 3 days, and then cell viability was measured with a colorimetric assay based on the use of 3-(4,5-dimethylthiazol-2-yl)-2,5-diphenyl tetrazolium bromide.³⁴ The results were read on a multiwell scanning spectrophotometer (AF2200 plate reader, Eppendorf, Milan, Italy), using a wavelength of 570 nm. Each value was the average of 6–8 wells. The 50% growth inhibition (GI₅₀) value was calculated according to the NCI (Bethesda, MD, USA):⁴⁶ thus, GI₅₀ is the concentration of test compound where 100(T – T₀)/(C – T₀) = 50 (where *T* is the optical density of the test well after a 72 h period of exposure to test compound, *T₀* is the optical density at time zero, and *C* is the DMSO control optical density). The cytotoxicity effect was calculated according to the NCI when the optical density of treated cells was lower than the *T₀* value using the following formula: 100(T – T₀)/T₀.

Cell Cycle Analysis. Cell cycle progression was evaluated by DNA flow cytometry, with PI used to stain cells. Caco-2 cells were cultured in six-well plates and treated with compound (±)-**21** and 5-FU. Cells were harvested by trypsinization after 24–36 h of treatment, washed in PBS, and cooled in 70% ethanol at 4 °C for at least 30 min. Cells were washed in PBS to remove the ethanol and incubated for 1 h at 37 °C in a PBS solution containing RNase A (final concentration 100 μg/mL; Bio Basic Inc., Markham, Ontario, Canada). Finally, PI was added (final concentration 50 μg/mL; Agros Organics, Geel, Belgium), and the cellular suspension was incubated for 1 h at 37 °C. The cellular suspension was analyzed on a flow cytometer (Amnis FlowSight Millipore, Merck KgaA, Darmstadt, Germany), and results were analyzed using Image Data Exploration and Analysis (IDEAS) software (Amnis part of EMD Millipore, Seattle, WA, USA).

Apoptosis Analysis. Apoptotic cell death was measured by flow cytometry (Amnis FlowSight Millipore) using Alexa Fluor 488 annexin V/dead cell apoptosis kit with Alexa Fluor 488 annexin V and PI for flow cytometry (V13241, Invitrogen, Monza MB, Italy) according to the manufacturer's instructions. The numbers of live (annexin negative/PI negative), early apoptotic (annexin positive/PI negative), and late apoptotic/necrotic (annexin and PI positive) cells were determined using IDEAS software (Amnis part of EMD Millipore).

■ ASSOCIATED CONTENT

📄 Supporting Information

The Supporting Information is available free of charge on the ACS Publications website at DOI: 10.1021/acs.jnatprod.6b00577.

ESIMS and ¹H and ¹³C NMR spectra for compounds **13**, **14**, **16**, **17**, **19**, **20**; ESIMS, ¹H,¹³C COSY, HSQC, and HMBC spectra for neolignanamides (±)-**21**–(±)-**28**; stacked plot of RP-18-HPLC–UV of (±)-**4** and (±)-**21**–(±)-**28** (PDF)

AUTHOR INFORMATION

Corresponding Author

*Tel (C. Spatafora): +39 095 7385015. Fax: +39 095 580138.

E-mail: cspatafo@unict.it.

Notes

The authors declare no competing financial interest.

ACKNOWLEDGMENTS

This research was supported by a grant of the University of Catania (FIR—"Finanziamento della Ricerca" 2014).

REFERENCES

- (1) Moss, G. P. *Pure Appl. Chem.* **2000**, *72*, 1493–1523.
- (2) Gordaliza, M.; Castro, M. A.; del Corral, J. M. M.; San Feliciano, A. *Curr. Pharm. Des.* **2000**, *6*, 1811–1839.
- (3) Damayanthi, Y.; Lown, J. W. *Curr. Med. Chem.* **1998**, *5*, 205–252.
- (4) Huang, X.-X.; Zhou, C.-C.; Li, L.-Z.; Peng, Y.; Lou, L.-L.; Liu, S.; Li, D.-M.; Ikejima, T.; Song, S.-J. *Fitoterapia* **2013**, *91*, 217–223.
- (5) Lee, S.; Song, I.-H.; Lee, J.-H.; Yang, W.-Y.; Oh, K.-B.; Shin, J. *Bioorg. Med. Chem. Lett.* **2014**, *24*, 44–48.
- (6) Cho, J. Y.; Baik, K. U.; Yoo, E. S.; Yoshikawa, K.; Park, M. H. *J. Nat. Prod.* **2000**, *63*, 1205–1209.
- (7) Ghisalberti, E. L. *Phytomedicine* **1997**, *4*, 151–166.
- (8) Pieters, L.; Van Dyck, S.; Gao, M.; Bai, R. L.; Hamel, E.; Vlietinck, A.; Lemièrre, G. *J. Med. Chem.* **1999**, *42*, 5475–5481.
- (9) Hu, Q.-F.; MU, H.-X.; Huang, H.-Y.; Lv, H.-Y.; Li, S.-L.; Tu, P.-F.; Li, G.-P. *Chem. Pharm. Bull.* **2011**, *59*, 1421–1424.
- (10) Pieters, L.; Debruyne, T.; Claeys, M.; Vlietinck, A.; Calomme, M.; Vandenberghe, D. *J. Nat. Prod.* **1993**, *56*, 899–906.
- (11) Apers, S.; Paper, D.; Burgermeister, J.; Baronikova, S.; Van Dyck, S.; Lemièrre, G.; Vlietinck, A.; Pieters, L. *J. Nat. Prod.* **2002**, *65*, 718–720.
- (12) Lin, S.-Y.; Ko, H.-H.; Lee, S.-J.; Chang, H.-S.; Lin, C.-H.; Chen, I.-S. *Chem. Biodiversity* **2015**, *12*, 1057–1067.
- (13) Sawasdee, K.; Chaowasku, T.; Lipipun, V.; Dufat, T.-H.; Michel, S.; Likhitwitayawuid, K. *Tetrahedron Lett.* **2013**, *54*, 4259–4263.
- (14) Ma, C. J.; Kim, S. R.; Kim, J.; Kim, Y. C. *Br. J. Pharmacol.* **2005**, *146*, 752–759.
- (15) Pickel, B.; Schaller, A. *Appl. Microbiol. Biotechnol.* **2013**, *97*, 8427–8438.
- (16) Sun, J.; Gu, Y.-F.; Su, X.-Q.; Li, M.-M.; Huo, H.-X.; Zhang, J.; Zeng, K.-W.; Zhang, Q.; Zhao, Y.-F.; Li, J.; Tu, P.-F. *Fitoterapia* **2014**, *98*, 110–116.
- (17) Ma, C. Y.; Liu, W. K.; Che, C. T. *J. Nat. Prod.* **2002**, *65*, 206–209.
- (18) Stoessl, A. *Tetrahedron Lett.* **1966**, *7*, 2849–2851.
- (19) Wakimoto, T.; Nitta, M. K. K.; Chiba, T.; Yiping, Y.; Tsuji, K.; Kan, T.; Nukaya, H.; Ishiguro, M.; Koike, M.; Yokoo, Y.; Suwa, Y. *Bioorg. Med. Chem. Lett.* **2009**, *19*, 5905–5908.
- (20) Di Micco, S.; Mazue, F.; Daquino, C.; Spatafora, C.; Delmas, D.; Latruffe, N.; Tringali, C.; Riccio, R.; Bifulco, G. *Biomol. Chem.* **2011**, *9*, 701–710.
- (21) Vijayakurup, V.; Spatafora, C.; Daquino, C.; Tringali, C.; Srinivas, P.; Gopala, S. *Life Sci.* **2012**, *91*, 1336–1344.
- (22) Vijayakurup, V.; Spatafora, C.; Tringali, C.; Jayakrishnan, P. C.; Srinivas, P.; Gopala, S. *Mol. Biol. Rep.* **2014**, *41*, 85–94.
- (23) Bhusainahalli, V. M.; Spatafora, C.; Chalal, M.; Vervandier-Fasseur, D.; Meunier, P.; Latruffe, N.; Tringali, C. *Eur. J. Org. Chem.* **2012**, *2012*, 5217–5224.
- (24) Spatafora, C.; Barresi, V.; Bhusainahalli, V. M.; Di Micco, S.; Musso, N.; Riccio, R.; Bifulco, G.; Condorelli, D.; Tringali, C. *Org. Biomol. Chem.* **2014**, *12*, 2686–2701.
- (25) Spatafora, C.; Daquino, C.; Tringali, C.; Amorati, R. *Org. Biomol. Chem.* **2013**, *11*, 4291–4294.
- (26) Basini, G.; Baioni, L.; Bussolati, S.; Grasselli, F.; Daquino, C.; Spatafora, C.; Tringali, C. *Invest. New Drugs* **2012**, *30*, 186–190.
- (27) Basini, G.; Spatafora, C.; Tringali, C.; Bussolati, S.; Grasselli, F. *J. Biomol. Screening* **2014**, *19*, 1282–1289.
- (28) Mogharabi, M.; Faramarzi, M. A. *Adv. Synth. Catal.* **2014**, *356*, 897–927.
- (29) Spatafora, C.; Tringali, C. In *Targets in Heterocyclic Systems. Chemistry and Properties*; Attanasi, O. A., Spinelli, D., Eds.; Società Chimica Italiana: Rome, 2007; Vol. *11*, pp 284–312.
- (30) Bruschi, M.; Orlandi, M.; Rindone, B.; Rummakko, P.; Zoia, L. *J. Phys. Org. Chem.* **2006**, *19*, 592–596.
- (31) Orlandi, M.; Rindone, B.; Molteni, G.; Rummakko, P.; Brunow, G. *Tetrahedron* **2001**, *57*, 371–378.
- (32) Seca, A. M. L.; Silva, A. M. S.; Silvestre, A. J. D.; Cavaleiro, J. A. S.; Domingues, F. M. J.; Neto, C. P. *Phytochemistry* **2001**, *58*, 1219–1223.
- (33) Li, S. M.; Iliefski, T.; Lundquist, K.; Wallis, A. F. A. *Phytochemistry* **1997**, *46*, 929–934.
- (34) Mosmann, T. *J. Immunol. Methods* **1983**, *65*, 55–63.
- (35) Giaginis, C.; Tsantili-Kakoulidou, A. *J. Liq. Chromatogr. Relat. Technol.* **2008**, *31*, 79–96.
- (36) Henchoz, Y.; Guillaume, D.; Rudaz, S.; Veuthey, J.-L.; Carrupt, P.-A. *J. Med. Chem.* **2008**, *51*, 396–399.
- (37) Drews, A.; Bovens, S.; Roebrock, K.; Sunderkoetter, C.; Reinhardt, D.; Schaefer, M.; van der Velde, A.; Elfringhoff, A. S.; Fabian, J.; Lehr, M. *J. Med. Chem.* **2010**, *53*, 5165–5178.
- (38) Berova, N.; Ellestad, G.; Nakanishi, K.; Harada, N. In *Bioactive Compounds from Natural Sources. Natural Products as Lead Compounds in Drug Discovery*, 2nd ed.; Tringali, C., Ed.; CRC Press-Taylor & Francis: Boca Raton, FL, 2012; Chapter 5, pp 133–166.
- (39) Di Micco, S.; Spatafora, C.; Cardullo, N.; Riccio, R.; Fischer, K.; Pergola, C.; Koeberle, A.; Werz, O.; Chalal, M.; Vervandier-Fasseur, D.; Tringali, C.; Bifulco, G. *Bioorg. Med. Chem.* **2016**, *24*, 820–826.
- (40) Lemièrre, G.; Gao, M.; Degroot, A.; Dommisse, R.; Lepoivre, J.; Pieters, L.; Buss, V. *J. Chem. Soc., Perkin Trans. 1* **1995**, 1775–1779.
- (41) Kurosawa, W.; Kobayashi, H.; Kan, T.; Fukuyama, T. *Tetrahedron* **2004**, *60*, 9615–9628.
- (42) Longley, D. B.; Harkin, D. P.; Johnston, P. G. *Nat. Rev. Cancer* **2003**, *3*, 330–338.
- (43) Yoshiharas, T.; Takamatsu, S.; Sakamura, S. *Agric. Biol. Chem.* **1978**, *42*, 623–627.
- (44) Wu, Y. C.; Chang, G. Y.; Ko, F. N.; Teng, C. M. *Planta Med.* **1995**, *61*, 146–149.
- (45) Barresi, V.; Trovato Salinaro, A.; Spampinato, G.; Musso, N.; Castorina, S.; Rizzarelli, E.; Condorelli, D. F. *FEBS Open Bio* **2016**, DOI: 10.1002/22111-5463.12060.
- (46) Scherf, U.; Ross, D. T.; Waltham, M.; Smith, L. H.; Lee, J. K.; Tanabe, L.; Kohn, K. W.; Reinhold, W. C.; Myers, T. G.; Andrews, D. T.; Scudiero, D. A.; Eisen, M. B.; Sausville, E. A.; Pommier, Y.; Botstein, D.; Brown, P. O.; Weinstein, J. N. *Nat. Genet.* **2000**, *24*, 236–244.